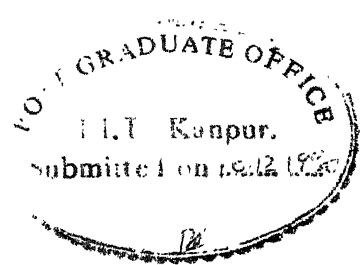


**RESONANCE SERIES AND ABSORPTION OF BROMINE
IN THE VACUUM ULTRAVIOLET AND RKR
POTENTIALS AND LONG-RANGE ANALYSES OF Br₂, Cl₂ AND I₂**

**A Thesis Submitted
in Partial Fulfilment of the Requirements
for the Degree of
DOCTOR OF PHILOSOPHY**

By
V. N. SARMA

**to the
DEPARTMENT OF PHYSICS
INDIAN INSTITUTE OF TECHNOLOGY, KANPUR
DECEMBER, 1980**



CERTIFICATE

This is to certify that the work presented in this thesis titled 'Resonance Series and Absorption of Bromine in the Vacuum Ultraviolet and RKR Potentials and Long-range Analyses of Br₂, Cl₂ and I₂' is the original work of Sri V. N. Sarma, done under my supervision and it has not been submitted elsewhere for a degree.

Putcha Venkateswarlu

(Putcha Venkateswarlu)

Department of Physics

Indian Institute of Technology,

Kanpur

December, 1980.

POST GRADUATE OFFICE

This thesis has been approved
for the award of the Degree of
Doctor of Philosophy (Ph.D.)
in accordance with the
regulations of the Indian
Institute of Technology, Kanpur

Dated: 12.4.1981

BP

PHY-1980-D-SHA-RES

I.I.T. KANPUR

GENERAL RECEIVED
Acc. No. A 65963

15 MAY 1981

ACKNOWLEDGEMENTS

I thank Professor P. Venkateswarlu for introducing me to the field of spectroscopy. I esteem him for his encouragement and interest both in my work and in me. I thank Dr. Y.V. Rao, for his valuable suggestions and Dr. (Mrs.) Sushama Tiwari for helping me with my computer work. I appreciate the help from friends Ms.T. Pramila and Mr. B.R. Reddy, and especially my brother Mr. V.N. Moorthy, in the preparation of the thesis. I thank Mr. H.K. Panda for cyclostyling the thesis. I thank Ms. Komala more than once for her invaluable help.

I thank National Bureau of Standards for general help and the INSA for a Research Fellowship.

Finally thanks to DEC-10 system without which it would not have been possible to realize this work.

V N Sarma

C O N T E N T S

Chapter 1	Introduction	1
	Potential energy curve	2
	Extrapolation of $G(v)$ and B_v	6
	Long-range Analysis	10
Chapter 2	Resonance Series of Bromine	
	Introduction	13
	Experiment	14
	Results	15
	Evaluation of J_r values	19
	Determination of Rotational Constants	21
	Vibrational Analysis	22
	Potential Energy Curve	25
	Upper State	26
	Conclusions	29
	Figures	30
	Tables	36
Chapter 3	Long-range analysis of the α and β states of Br_2	
	Introduction	50
	The Long-range Analysis of α State $^{79,81}Br_2$	50

B $^3\Pi$ (Σ_u^+) of $^{79}\text{Br}_2$	54
Figures	56
Tables	57
Chapter 4 Long-range Analysis of Cl_2 and I_2	
B $^3\Pi$ (Σ_u^+) State of Cl_2	61
X $^1\Sigma_g^+$ State of Chlorine	63
I $^1\Sigma_g^+$ State of Iodine	65
Long-range Analysis	66
Figures	71
Tables	76
Chapter 5 Absorption Spectrum of Bromine in the Vacuum Ultraviolet	
Tables	99
Bibliography	103

CHAPTER 1

INTRODUCTION

Molecular spectra are perhaps the most important means of investigating molecular structure.²⁰ They give direct information on the various discrete energy levels of a molecule. Also, they give detailed information about the motion of electrons (electronic structure) and vibration and rotation of nuclei in the molecule. From the vibrational frequencies, the forces between the atoms in the molecule can be calculated with great accuracy. These forces may be divided into four types: 1. short-
2. intermediate- 3. long- and 4. very long-range forces.^{1,2,3} It is the third type viz. long-range forces with which the present exposition is concerned with. The long-range analysis of halogens (Br_2 , Cl_2 , I_2) is presented in this thesis.

It is the purpose of this chapter to introduce the background of long-range analysis necessary to understand the following chapters. In the long-range analysis, the potential coefficients are calculated using the outer turning points of the RKR potential. It is necessary to compute the potential upto dissociation for such a calculation. For computing the potential upto dissociation, energy levels near dissociation limit (which are rarely observed⁴) are extrapolated using theoretical methods. The details of computation of RKR potentials, the methods of extrapolation of energy levels and the long-range analysis are presented

here in the following.

Potential Energy Curve

The spectroscopic data on energy levels may be used to obtain several types of potential functions,^{13,23} which are useful for a semi quantitative discussion, but may be badly in error at high vibrational levels.

A much better procedure is to employ the Rydberg-Klein-Rees (RKR) first order WKB method in which no special assumptions about the mathematical form of the potential are made. The experimentally known energy levels are used to calculate the points on the potential curve corresponding to the classical turning points of nuclear motion. The method was devised by Rydberg,¹⁴ and Klein¹⁵ on the basis of Bohr-Sommerfield quantisation of the phase integral for the vibrational motion. Rees¹⁶ developed analytical modifications to their graphical procedures. Vanderslice et al.¹⁷ made it compatible for use on high speed electronic computers. This has now become fairly routine and has been adopted by a host of workers too numerous to enumerate here. Higher order WKB approximations have been studied and it has been shown that they are small even in the case of hydrogen.¹⁸

The method has a simple interpretation.^{17,19} The two quantum conditions required to evaluate the two classical turning points r_1 and r_2 of the vibrational motion

at a given experimental energy E , may be represented in terms of the area enclosed by the constant energy line E and the potential energy curve $U(r)$. The area A (fig.1.1) is given by

$$A = \int_{r_1}^{r_2} (E - U) dr \quad (1.1)$$

$$\text{where } U = V(r) + K/r^2 \quad (1.2)$$

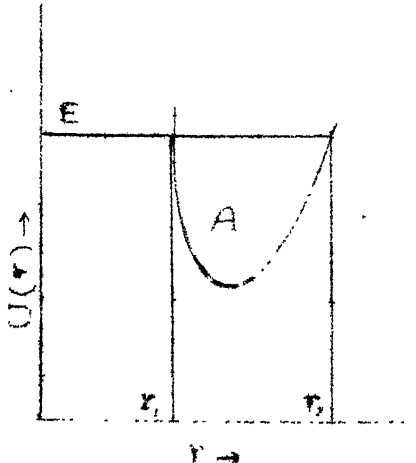


Fig.1.1

K/r^2 is the centrifugal energy.

It follows that

$$\begin{aligned} f(r) &= \left(\frac{\partial A}{\partial E}\right)_K = \int_{r_1}^{r_2} dr = r_2 - r_1 \\ g(r) &= -\left(\frac{\partial A}{\partial K}\right)_E = - \int_{r_1}^{r_2} \frac{dr}{r^2} \\ &= \frac{1}{r_1} - \frac{1}{r_2} \end{aligned} \quad (1.4)$$

Since E and K are related to vibrational rotational energies, A is expressed in terms of experimental energy levels to solve the problem. Using the action integral

$$\frac{dI}{dE} = \frac{\mu}{2} \int \frac{dr}{(E-U)^{1/2}} \quad (1.5)$$

Let I' be the value for which $E(I', K) = U$. It can be shown that

$$A = (2/\pi\mu^2)^{1/2} \int_0^{I'} (E-U)^{1/2} dI \quad (1.6)$$

For a rotationless state with $I = (v+\frac{1}{2})h$ (Bohr-Sommerfield quantisation rule), the following relations for the integrals f and g may be derived

$$f(r) = S \int_{-\frac{1}{2}}^V dv' / [V - g(v')]^{\frac{1}{2}} \quad (1.7)$$

$$g(r) = (1/S) \int_{-\frac{1}{2}}^V -\frac{B_v}{[V - g(v')]^{\frac{1}{2}}} dv' \quad (1.8)$$

where $S = (n/8\pi^2 c \mu)^{\frac{1}{2}}$, $G(v')$ are vibrational term values and B_v are rotational constants. v is the vibrational quantum number for which $V(r) = G(v)$. These integrals have a singularity at the upper limit. Rees overcame this difficulty by using an analytical expression for the observed energy levels. It involves the representation of vibrational energies by quadratics in $(v+\frac{1}{2})$. However, for most molecules, vibrational energies to a high v can never be represented by such quadratics. Vanderslice et al.¹⁷ introduced the method of representing the energy $E(I, K)$ by a series of quadratics $E_i(I, K)$. The following relations for f and g are derived.

$$f_n = S \sum_{i=1}^n -\frac{\log w_i}{(wx_i)^{\frac{1}{2}}} \quad (1.9)$$

$$g_n = (1/S) \sum_{i=1}^n [2\alpha_i (wx_i)^{-1} \{ (V_n - V_{i-1})^{\frac{1}{2}} - (V_n - V_i)^{\frac{1}{2}} \} + (1/\sqrt{wx_i}) \{ 2B_i - (\alpha_i w_i / wx_i) \} \log w_i] \quad (1.10)$$

where

$$w_i = \left| \frac{[w_i^2 - 4wx_i V_i]^{\frac{1}{2}} - 2[wx_i(V_n - V)]^{\frac{1}{2}}}{[w_i^2 - 4wx_i V_{i-1}]^{\frac{1}{2}} - 2[wx_i(V_n - V_{i-1})]^{\frac{1}{2}}} \right|$$

where wx_i , w_i , B_i and α_i are effective constants for the 'i'th segment of the quadratic fitting. V_i and V_{i+} are measured from the potential minimum. They are determined by fitting $G(v)$ and B_v of v and $v-l$ levels to the expressions

$$\begin{aligned} G(v) &= w_i (v+\frac{1}{2}) - wx_i (v+\frac{1}{2})^2 \\ B_v &= B_i - \alpha_i (v+\frac{1}{2}) \end{aligned} \quad (1.11)$$

However, the method is not sufficiently accurate near the upper limit of integration. Hence, f and g are calculated by this method only upto $v-6$ and from $v-6$ to v by a separate analytical method.⁸ The integrals from $v-6$ to $v-4$ and $v-4$ to $v-2$ are evaluated by fitting $\left[\frac{v}{G(v)} - \frac{v'}{G(v')} \right]^{\frac{1}{2}}$ to quadratics in $(v-v')$. The contribution from $v-2$ to v is obtained by a similar fitting to a cubic. Similar expressions also apply to $\int B_v dv' / [G(v)-G(v')]^{\frac{1}{2}}$. The method is quite accurate and competes with any of the numerical methods.

It is observed that the RKR potential at very high vibrational levels misbehaves, the repulsive branch of the potential either turns in or out. This results from the inaccurate molecular constants.^{6,28} In the RKR potential calculation, vibrational constants determine the width of the potential and rotational constants determine the absolute position of the turning points. More specifically, the smaller vibrational spacings give larger widths, and smaller B_v

give larger absolute turning points for the potential.

Yet a good approximation⁶ for the inner wall in this region may be obtained by an extrapolation from the region where the potential behaves well. The inner wall is fitted to the expression

$$V(r) = (a/r^{12}) + b \quad (1.12)$$

and the turning points were extrapolated using the $G(v)$ s. The outer wall was computed then using the widths determined from RKR potential. It was shown that the errors involved in estimating turning points are:

$$\begin{aligned} \delta(r_1 - r_2) &\approx -\delta(\Delta G_{v-\frac{1}{2}})/\Delta G_{v-\frac{1}{2}} \\ \delta(r_1 + r_2) &\approx -\frac{\delta B_v}{B_v} 1/2 [r_1 + r_2] \end{aligned} \quad (1.13)$$

Extrapolation of $G(v)$ and B_v

Since energy levels upto dissociation are rarely observed, usually they are obtained by extrapolation. Until recently, a linear extrapolation of the Birge-Spooner plot was the choice for such an extrapolation. But it is known that these plots show a positive curvature near dissociation limit and hence the extrapolated energy levels are less certain.

A more accurate method based on WKB approximation was developed by Le Roy and Bernstein.¹⁷ The WKB quantum condition for the eigen values of a potential $V(r)$ is

$$\int_{r_1}^{r_2} [G(v) - V(r)]^{\frac{1}{2}} dr = \pi\hbar/(2\mu)^{\frac{1}{2}} (v+\frac{1}{2}) \quad (1.14)$$

As indicated earlier, $V(r)$ may be represented in inverse powers of r , for large r .

$$V(r) = D - \sum_m C_m / r^m \quad (1.15)$$

where D is the dissociation limit. Over any small interval of r , the inverse power series may be approximated by a single 'effective' or 'local' term, C_n / r^n which is the weighted average of different terms and eq.1.15 becomes

$$V(r) = D - C_n / r^n \quad (1.16)$$

$$\text{where } n = \frac{\sum_m (m+1) m C_m / r^{m+1}}{\sum_m m C_m / r^{m+1}} \quad (1.17)$$

In the limit r reaches the asymptotic region, the noninteger n becomes \bar{n} (asymptotic value), the effective smallest integer power contribution to eq.1.15. Rearranging eq.1.14 and differentiating with respect to $G(v)$

$$\frac{dv}{dG(v)} = \frac{\sqrt{\mu/2}}{\pi\hbar} \int_{r_1}^{r_2} [G(v) - V(r)]^{-\frac{1}{2}} dr \quad (1.18)$$

Substituting eq.1.16 and setting $r_1 = 0$, eq.1.18 becomes upon integration

$$\frac{dG(v)}{dv} = K_n [L - G(v)]^{(n-2)/2n} \quad (1.19)$$

K_n is a constant involving gamma function. Integrating eq.1.19

$$G(v) = D - [(v_D - v) H_n]^{2n/(n-2)} \quad (1.20)$$

where $H_n = [(n-2)/2n]K_n$ and v_D is a constant. For $n > 2$ it becomes the effective vibrational index at which molecule dissociates. It can be shown¹⁰ that positive curvature of a Birge-Spooner plot is a necessary condition for the applicability of the above equations. Another useful relation may be obtained by using

$$\frac{dG(v)}{dv} \approx \Delta G_v = 1/2 [G(v+1) - G(v-1)] \quad (1.21)$$

in eq.1.19,

$$G(v) = D - K(\Delta G_v)^{2n/(n-2)} \quad (1.22)$$

$$\text{where } K = [1/K_n]^{2n/(n-2)}$$

In the present work, the values of D are accurately known. The asymptotic value of n for the state under study may be determined from linear fits of the observed $G(v)$ and ΔG_v to eq.1.22. The $G(v)$ may be then extrapolated

from eq.l.20, in which the constants v_D and H_n are obtained from a fit to the linear form of eq.l.20

$$[D - G(v)]^{(n-2)/2n} = (v_D - v) H_n \quad (l.23)$$

Replacing $V(r)$ in eq.l.14 by effective potential including centrifugal term, one may derive an expression⁷ for

$$B_v = Q_n (v_D - v)^{4/(n-2)} \quad (l.24)$$

where Q_n is a constant related to C_n . This expression is used in extrapolation of B_v over the tail of the potential curve.

It should be remembered that at shorter distances, exponential type of forces (exchange forces) replace the inverse power terms and hence the above treatment should be applied only to the long-range region where Birge-Spooner plots show positive curvature (the region where inverse power terms dominate). The integrand of eq.l.18 is over estimated as a result of setting $r_1 = 0$; consequently n and C_n determined thus are somewhat too large. Another source of error arises from the approximation of the sum of inverse power terms representing the potential by a single term (eq.l.15 by eq.l.16). This has the effect opposite to the above and the constants n and C_n thus determined are slightly too small. The eq.l.24 for the extrapolation of B_v values is less rigorous than the eq.l.22 for the

vibrational term values. The errors are introduced for the same reasons as those for the vibrational problem; only that they are more serious for the rotational constants. The values of B_v so determined are the upper bounds of the true values. The value of D obtained from the fits to eq. 1.22 is an upper bound, as the slope decreases with increasing n which is the case for lower levels. This is the result of approximating eq. 1.15 by eq. 1.16.

Long-range Analysis

In the beginning, only the first coefficient in the expansion of potential by inverse power series, has been determined and all higher contributions have been neglected. The constant C_n ($n = 5$ for B-states and 6 for X state halogens^{5,39}) has been determined from the linear fits of $[D - G(v)]^{(n-2)/2n}$ and v . The constant H_n in eq. 1.20 is related to C_n by

$$\bar{H}_n = \frac{\bar{H}_n}{[\sqrt{\mu} C_n^{1/n}]} \quad (1.25)$$

\bar{H}_n is a constant depending on n . The potential expansion may be rewritten as

$$D - G(v) = \sum_n C_n / r^n \quad (1.26)$$

Joscinski developed a method in which the first two terms in eq. 1.26 are directly determined implicitly considering the

higher terms. His equation determining the first two C_n is

$$[D - G(v)]r^{-6} = C_6 [1 - (C_8/C_6)r^{-2}]^{-1} \quad (1.27)$$

in which C_{10} becomes equal to C_8^2/C_6 . Eq.1.27 may be generalised⁹ by using the following equations

$$[D - G(v)]r^{n1} = C_{n1} [1 - \alpha(C_{n2}/C_{n1})r^{n2-n1}]^{-1/\alpha} \quad (1.28)$$

This equation gives simple two term expansion for $\alpha = -1$ and Goscinski's for $\alpha = +1$. C_{n3} in eq.1.26 is given by

$$C_{n3} = 1/2 (1 + \alpha) C_{n2}^2/C_{n1} \quad (1.29)$$

with the assumption $n_3 = 2n_2 - n_1$ which is true for second order perturbation energies i.e. $n = 6, 8, 10, \dots$. Eq.1.28 may be rearranged to a linear version

$$\{r^{n1} [D - G(v)]\}^{-\alpha} = C_{n1}^{-\alpha} - [\alpha C_{n2}/C_{n1}]^{(1+\alpha)}/r^{n2-n1} \quad (1.30)$$

and for the case $\alpha = 0$

$$\log \{ r^{n1} [D - G(v)] \} = \log (C_{n1}) + (C_{n2}/C_{n1})/r^{n2-n1} \quad (1.31)$$

A prior knowledge of any of the force constants may be utilized by replacing

$$[D - G(v)] \text{ with } [D - G(v) - C_n/r^n] \quad (1.32)$$

in eqs. 1.30 and 1.31. Eq.1.26 may also be rearranged to give a linear equation as

$$R^{m+3} [D - G(v)] = \sum_K C_K R^K \quad (1.33)$$

where $R = r^2$ and $\lambda = 2(m + 3 - K)$

$$\lambda = 0 \text{ to } m$$

Eq. 1.33 is also applied in the analysis to obtain C_6 , C_8 and C_{10} which are compared then with those obtained from eqs. 1.30 and 1.31. The applicability of these methods is restricted to $r_b(\text{ab}) \geq 2 [\langle r_A^2 \rangle^{\frac{1}{2}} + \langle r_B^2 \rangle^{\frac{1}{2}}]$ for the interaction of two atoms A and B. Here $\langle r_x^2 \rangle$ is the expectation value of the square of the radius of the outermost electrons on atom x. The reason is that the overlap of electron clouds of two atoms increases so much as to break down the inverse power expansion. The values of r_b are calculated for X and B states of halogens from the expectation values of the orbitals⁵⁰ and are given in tables 4.7 and 4.9.

As will be seen later in chapter 4, the utility of Le Roy and Bernstein's approach for the extrapolation of energies near dissociation is great. Also, the long-range constants obtained from his method are compatible with those obtained from eqs. 1.32 and 1.33.

CHAPTER 2

RESONANCE SERIES OF BROMINE

Introduction

Resonance fluorescence spectrum of Br_2 was first recorded by Rao and Venkateswarlu²⁵ in the region 1565-1860A. They observed a series of doublets excited by the bromine atomic line 63497.8 cm^{-1} . These doublets correspond to vibrational levels ranging from $v = 4$ to 36 of the ground state. Using the absorption data,²⁴ they calculated the molecular constants of the ground state of bromine molecule. Using the absorption²⁶ and the fluorescence data, Le Roy and Burns²⁸ tried to improve these molecular constants following an iterative method based on RKR potential, the reliability of which was doubtful according to Coxon²⁷. Coxon²⁷ from the analysis of the B-X system of $^{79}\text{Br}_2$ in absorption, reported the molecular constants for $0 \leq v \leq 10$. Also, he computed the potential curve using his data for $v = 0$ to 10 and the fluorescence data above $v = 10$ upto 36. Barrow et al.²⁹ from a study of the absorption spectra of $^{79}\text{Br}_2$ and $^{81}\text{Br}_2$, improved the molecular constants for $0 \leq v \leq 10$, in which rotational constants for $v = 0$ and 1 have been determined by a cyclic process.³⁰

Here, the notation of Herzberg²⁰ is followed except that no primes are used to denote the lower state quantities.

It is clear that, on the whole, no reliable data exists for the ground state of bromine above $v = 10$. To make up for this deficiency, an analysis of the vacuum ultraviolet resonance series of Br_2 in the region of 1500-2100 Å taken in high resolution is undertaken in the present work.

Experiment *

The resonance doublets of Br_2 were excited by microwave diathermi source at 2400 MHz. The doublets could be obtained relatively free of background by adjusting the pressure of He and Br_2 in the cell. The spectrum was photographed with a 10.6 m concave grating spectrograph in the region 1500-2100 Å in 6th and 7th orders at a dispersion varying between 0.21 Å/mm to 0.29 Å/mm. The spectra were recorded on Ilford Q₂ plates. Iron lines in 2nd and 3rd orders were used as standards. The wave numbers of all spectral lines were obtained using a large number of standard lines by least-squares method programmed in FORTRAN-10. The accuracy of the measurements is about $\pm 0.06 \text{ cm}^{-1}$.

* The spectra are taken by Professor P. Venkateswarlu in Ottawa, Canada as high resolution facilities are not available in this country.

Results

The spectrum showed several long progressions of doublets in the region 1500-2100 Å. The doublets repeat at gradually decreasing intervals and proceed to converge to different limits. The intervals between adjacent members of the series correspond to the vibrational quanta of the ground state, $\chi \Sigma_g^+$ of $^{79,81}\text{Br}_2$. Twelve different series named A_1 , A_2 , A_3 , A_4 , B_1 , B_2 , C , D , E_1 , E_2 , G_1 and G_2 could be definitely identified and analysed (tables 2.1 to 2.6). In addition there are members of a few other series which are weaker and are not studied in the present work. The series A^* and B are strong and the series C , G , E and D are of intermediate intensity. The doublets identified correspond to v values from 0 to 36 for series A , C and G , from 13 to 76 for series B , from 1 to 65 for series D and from 25 to 71 for series E . Four bromine atomic lines, 63436.52cm^{-1} , 63498.51cm^{-1} , 64907.24cm^{-1} and 65285.18cm^{-1} excite the molecules initially from either $v = 0$ or 1 of the ground state to some rotational (designated by J_r) vibration level of an upper electronic state. The observed resonance doublets result from the reverse transitions to various vibrational levels of the ground state.

* Series A_1 , A_2 , A_3 and A_4 are collectively referred to as series A and also similar notation for other subscripted series is used, in this chapter.

Among these doublet series, some pairs ($A_1 - A_2$, $A_3 - A_4$, $B_1 - B_2$, $G_1 - G_2$ and $E_1 - E_2$) were detected each of which has the same upper vibronic level excited by the same resonance line. The upper state rotational quantum numbers for such pairs differed by 3 units. The relative position of the doublets of these pairs in the spectrum gives the appearance of quartets and henceforth such pairs are termed quartet series. The origin and the relative positions of the doublets of the quartet series are shown in figs. 2.1-2.3. The resonance line 63498.51 cm^{-1} excites the molecules from $v = 1$ of the ground state to the upper vibronic level from which the quartets $A_1 - A_2$ originate, with J_r values equal to 58 and 55 respectively. The resonance line coincides with R line and with P line of $v = 1$ doublets respectively for A_1 and A_2 . Similarly the resonance line 63498.51 cm^{-1} is responsible for the quartet series $A_3 - A_4$. Here, this resonance line coincides with R line for A_3 series, while it coincides with P line for A_4 series. Again the lower state is $v = 1$ of the ground state, with J_r values 68 and 65 respectively for A_3 and A_4 series.

Similar observations were made for the other quartet series $B_1 - B_2$, $E_1 - E_2$ and $G_1 - G_2$. The resonance line excites molecules from $v = 0$ of the ground state. Figs. 2.1-2.3 explain the process of excitation while table 2.7 gives the frequencies of the exciting

lines, the values of J_r , and lower state quantum numbers for all the series.

The atomic line 64907.24 cm^{-1} raises the molecules from $v = 0$ to a rovibronic level with $J_r = 45$, from which the doublet series C originates. Here, the atomic line coincides with R line of the $v = 0$ doublet. Similarly, 63436.52 cm^{-1} gives rise to series D, for which J_r is 51. In all the above quartet series the middle lines overlap each other for lower vibrational levels, and hence give the appearance of triplets. These were resolved beyond $v = 17$ for $A_1 - A_2$, $v = 16$ for $A_3 - A_4$, $v = 10$ for $G_1 - G_2$ series respectively. No such triplets were identified for B and E series. Some of the members of these series were weak or missing in accordance with Frank-C Condon principle.

When the lines R₁ and P₂, (shown in figs. 2.1-2.3) coincide, one has

$$\Delta F' = F'_v (J_r + 3) - F_v (J_r) = F_v (J_r + 2) - F_v (J_r + 1) \quad (2.1)$$

$$= (J_r + 2) [2B_v - 4D_v (J_r + 2)^2] \quad (2.2)$$

where F and F' are the rotational term values of the lower and upper states. Neglecting D_v for a first approximation, the eq. 2.1 gives

$$6B_v (J_r + 2) \approx 2B_v (J_r + 2) \quad (2.3)$$

$$\text{or } B'_v \approx 1/3 B_v \quad (2.4)$$

At this point it is interesting to note that the components of the quartet change their position, with increasing v . Following the notation that $\delta(R_1 P_2)$ is the separation between the components R_1 and P_2 of the quartet, we have

$$\begin{aligned}\delta(R_1 P_2) &= [6(B_v^! - 4D_v^!) (J_r + 2) - 12D_v^! (J_r + 2)^3] \\ &\quad - [2B_v^! (J_r + 2) - 4D_v^! (J_r + 2)^3]\end{aligned}\quad (2.5)$$

$$\begin{aligned}\delta(R_2 P_1) &= 10(J_r + 2) [B_v^! - 2D_v^! (J_r^2 + 4J_r + 10)] \\ &\quad - [(6B_v^! - 4D_v^!) (J_r + 2) - 12D_v^! (J_r + 2)^3]\end{aligned}\quad (2.6)$$

The above equations indicate that with increasing v , the total width of the quartet goes on decreasing, the blended middle components separate out ; R_2 and R_1 coincide following which P_2 and P_1 coincide; then the doublets are reversed i.e. the order of the lines change to P_2 , P_1 , R_2 , R_1 , the total width being $\delta(R_1 P_2)$ at this point. (Fig. 2.2) When R lines coincide,

$$\begin{aligned}F_v^! (J_r + 2) - F_v^! (J_r - 1) &= \Delta F^! \\ \text{i.e. } 6(B_v^! - 4D_v^!) 12 D_v^! (J_r + 1)^2 &= \Delta F^! / (J_r + 1)\end{aligned}\quad (2.7)$$

When P lines coincide,

$$\begin{aligned}F_v^! (J_r + 4) - F_v^! (J_r + 1) &= \Delta F^! \\ \text{or } 6(B_v^! - 4D_v^!) 12 D_v^! (J_r + 3)^2 &= \Delta F^! / (J_r + 3)\end{aligned}\quad (2.8)$$

Supposing $D_v^!$ can be neglected in eqs. 2.7 and 2.8 the

values of B_v for the two cases would almost be the same i.e. the two doublets R_2P_2 and R_1P_1 may be assumed to coincide. This gives

$$12B_v - 72 D_v (J_r^2 + 4J_r + 5) = 0 \quad (2.9)$$

The eq. 2.9 with either eq. 2.7 or eq. 2.8 gives B_v a value, 0.040276cm^{-1} which corresponds to the vibrational level 69 for B series. Neglecting b_v , the above equations give a value of B_v which is $1/3$ of that for $v = 0$, corresponding to the vibrational level 75. However, in the present spectra, such a doublet was not exactly observed but estimated to occur between 73 and 74. A totally reversed quartet was identified at $v = 75$.

The closeness of the values of v (69 or 75) calculated above with the estimated $v = 73$ from observation is satisfactory, the difference may be partly due to the approximation of the eqs. 2.7-2.9 in which the higher order terms are neglected.

Evaluation of J_r values

The doublet separation δv of a series is given by

$$\delta v = (4 J_r + 2) [B_v - 2D_v (J_r^2 + J_r + 1)] \quad (2.10)$$

J_r is the rotational level in the upper state and B_v and D_v are rotational constants of the ground state. Expressing

B_v and D_v as polynomials in $(v+\frac{1}{2})$

$$B_v = B_e - \alpha_e(v+\frac{1}{2}) + \gamma_e(v+\frac{1}{2})^2 + \delta_e(v+\frac{1}{2})^3 + \varphi_e(v+\frac{1}{2})^4 \quad (2.11)$$

$$D_v = D_e + \beta_e(v+\frac{1}{2}) \quad (2.12)$$

Substituting eqs. 2.11 and 2.12 in eq. 2.10

$$\delta v = (4J_r + 2)[B_e - 2D_e(J_r^2 + J_r + 1) + \{-\alpha_e + 2\beta_e(J_r^2 + J_r + 1)\}x(v+\frac{1}{2}) + \gamma_e(v+\frac{1}{2})^2 + \delta_e(v+\frac{1}{2})^3 + \varphi_e(v+\frac{1}{2})^4] \quad (2.13)$$

Plots of δv vs $(v+\frac{1}{2})$ are drawn and smooth δv were obtained for different lower values of v . Using these δv values along with B_v values calculated from the work of Barrow et al.,²⁹ J_r for all series were initially obtained from eq. 2.10 neglecting D_v . These J_r values so obtained are found to be consistent with those obtained from detailed calculations made in the following manner.

Making use of the graphs, fig. 2.4 and 2.5, the points of large scatter are omitted while least square fitting the values of δv to eq. 2.13 by fourth degree polynomials of the form

$$\delta v = a_0 + a_1(v+\frac{1}{2}) + a_2(v+\frac{1}{2})^2 + a_3(v+\frac{1}{2})^3 + a_4(v+\frac{1}{2})^4$$

$$\text{or in short } \delta v = \sum_n a_n(v+\frac{1}{2})^n; \quad n = 0 \text{ to } 4 \quad (2.14)$$

Comparing eq. 2.13 and eq. 2.14,

$$\begin{aligned} a_0 &= (4J_r + 2)[B_e - 2D_e(J_r^2 + J_r + 1)] \\ a_1 &= (4J_r + 2)[-a_e + 2\beta_e(J_r^2 + J_r + 1)] \\ a_2 &= (4J_r + 2)\gamma_e; \quad a_3 = (4J_r + 2)\delta_e; \quad a_4 = (4J_r + 2)\varphi_e \end{aligned} \quad (2.15)$$

The coefficients $[a_n]$ of each series are determined from separate least squares fits. The series A, C, G and D (upto $v = 32$) require only second degree polynomials, which means $a_3 = a_4 = 0$ in eq. 2.14. Neglecting D_e from the first of eq. 2.15

$$a_0 = (4J_r + 2)B_e \quad (2.16)$$

Using the value of B_e , from the work of Barrow et al.,²⁹ J_r is calculated for all series. The values of a_0 and J_r for all series are listed in table 2.7.

Determination of Rotational Constants

The rotational constants were obtained from eq. 2.15 in two stages. In the first, a preliminary set of molecular constants for A, C, D, G series were obtained as follows. As, either some of the doublets or components of the doublets are missing, the doublet separations calculated from the molecular constants²⁹ were used in place of missing experimental values between $v = 0$ and 4. Then series, A, C, D, G in all eight, were separately fitted to polynomials of type eq. 2.14 yielding the coefficients $[a_n]$ for each series. The first two of eqs. 2.15 can be rewritten as

$$\begin{aligned} B_e - K D_e &= a_0 / (4J_r + 2) \\ - \alpha_e + K \beta_e &= a_1 / (4J_r + 2) \end{aligned} \quad (2.17)$$

where $K = 2(J_r^2 + J_r + 1)$, the independent variable. As it is an over determined problem, the constants were calculated by least squares treatment of eq. 2.16, with $[a_n]$ as functions of K. The mean values of the constants γ_e , δ_e , φ_e were obtained from the last three of eqs. 2.15. The molecular constants so obtained are all listed in table 2.9. These constants were used to calculate $\delta\nu$, the doublet separation for all series upto $v = 36$. The difference between calculated and observed $\delta\nu$, varies between 0.04 to 0.07cm^{-1} .

In the second step the gaps in series E, D and B upto $v = 36$ were filled with the above $\delta\nu$'s, and the data was subjected to the least squares analysis once more exactly as before, to get the coefficients $[a_n]$ for each of the series E, D and B. The least squares treatment of the coefficients $[a_n]$ gave molecular constants which represent the entire range i.e., $v = 0$ to 70. As a check, $\delta\nu$'s with these constants were calculated which agree well with observed doublet separations within $\pm 0.10\text{cm}^{-1}$. The constants are listed in table 2.9.

Vibrational Analysis

The rotational term values of the ground state corresponding to all series for both P and R branches were calculated using the rotational constants and the J_r 's. The position of the upper rovibronic level $T(J_r)$ is

obtained by the following expressions

$$T(J_r) = \text{Resonance line} + F_v(J) + G_o(v) \quad (2.18)$$

$G_o(v)$ is the vibrational term value and $F_v(J)$ is the rotational term value of the lower state and $J = J_r \pm 1$ according as the resonance line coincides with P or R line of level v from which the molecules are initially excited, v is '1' for series A and '0' for all others. $G_o(v)$, the vibrational term values of $X^1\Sigma_g^+$ are given by

$$G_o(v) = T(J_r) - E(v) \quad (2.19)$$

where $E(v)$ is the sum of the frequency of the transition to the level v and the rotation term value $F_v(J)$, which has the same meaning as in eq. 2.18.

There is a difficulty involved in determining $G_o(v)$ from this method. As the resonance lines have large widths, the calculated $T(J_r)$ and hence $G_o(v)$ would be less accurate. However, this was over come by using $G_o(v)$'s from an earlier work. Vibrational spacings for λ state of bromine are accurately known upto $v = 10$.²⁹ Coupling this information to the observed line frequencies, $T(J_r)$ was calculated from eq. 2.19. Neglecting the widely differing values, an average $T(J_r)$ was calculated for each of the series. These are given in table 2.10. The vibrational term values for the ground state from all observed lines are then calculated using eq. 2.19. It was, then, observed that the average $G_o(v)$ of P and R branches of

one series differed from another by approximately constant amounts. The explanation is : the resonance lines being very broad, the exact separation of the higher and lower energy levels does not correspond to the centre of the line which is measured, but to a value differing from the centre by $\pm \Delta$. The Δ 's for all series were determined by comparing the present vibrational term values with those of the earlier work²⁹ and given in table 2.7.

As vibrational levels only upto $v = 10$ are available accurately, the $G_0(v)$ values in the present work were obtained in three stages : i) an internal standard was developed by comparing the average $G_0(v)$ of A_1 and A_2 with those of Barrow et al.²⁹ ii) the series A_3 , A_4 , C, G_1 and G_2 were compared with the above internal standard and the Δ 's determined. The average of all these series fixes the vibrational levels upto $v = 36$. iii) the Δ 's for series B_1 , B_2 , D, L_1 and E_2 were then determined likewise by comparing the levels upto 36 with those determined in step (ii). At this stage an average of these series gives the vibrational energies for the entire range of v . These are given in table 2.8.

From here it is a straight course to determine the vibrational constants. The term values from $v = 4$ to 32 are least squares fitted to polynomials,

$$G_0(v) = \sum_n b_n v^n, \quad n = 0 \text{ to } 3 \quad (2.20)$$

where the coefficients $[b_n]$ give w_0, w_0x_0, w_0y_0 and w_0z_0 as n varies from 0 to 3 respectively. The constants are given in table 2.9. Along with the vibrational constants w_e, w_ex_e, w_ey_e and w_ez_e were determined from the interrelationships with the above constants.²⁰ Calculated from these constants, the zero point energy is 161.405cm^{-1} . Vibrational term values. $G_e(v)$ were obtained by adding the above zero point energy. $G_e(v)$ for $v = 1$ to 3 calculated from the above constants, were used in fitting the data in the following. The vibrational term values $G_e(v)$ could not be fitted over the entire range i.e. $v = 0$ to 76, by a single polynomial in $(v+\frac{1}{2})$. The values for $0 \leq v \leq 60$ have been fitted by least squares to the expression

$$G_e(v) = \sum_n C_n (v+\frac{1}{2})^n, \quad n = 0 \text{ to } 6 \quad (2.21)$$

to an accuracy of $\pm 0.07\text{cm}^{-1}$ and the coefficients are presented in table 2.9. $G_e(v)$ for $v = 60$ to 75 were smoothed by fitting them to a polynomial in $(v+\frac{1}{2})$.

Potential Energy Curve

As mentioned in the first chapter several methods of computation of potentials are available. However, only the RKR method is used to obtain the potential energy curve in the present work. The curve

is calculated using a standard program which requires spectroscopic constants ($w_e x_e$, w_e , α_e and B_e), $G_e(v)$ and B_v values, as input. The term values, from $v = 0$ to 60 smoothed by least squares method were used in the program. The turning points are listed in table 2.8. The repulsive branch of the curve turns inward above $v = 64$ which is not unexpected.⁶ Hence the potentials are corrected above $v = 60$ and the long-range analysis is carried out as given in the next chapter.

Upper State

It is usually difficult to obtain useful information about the upper state from resonance fluorescence. However, as there are seven excited levels covering a region 2000cm^{-1} in their T_v values, efforts are made to extract some information. Of the twelve resonance series only five quartet series give significant information about the upper state.

An estimate of the rotational constant, B_{eff} is obtained from the quartet series, mentioned earlier in this chapter. Rearranging eq. 2.6,

$$\Delta F' = E'_v(J_r+3) - E'_v(J_r) = 10(J_r+2)[B_v - 2D_v(J_r^{\frac{2}{2}} + 4J_r + 10)] - \delta(R_2 P_1) \quad (2.22)$$

where J_r belongs to the vibrational level v' of the upper state. The rotational term value of the J_r th level is

$$F_v' (J_r) = [B_v' - D_v' J_r (J_r + 1)] J_r (J_r + 1) \quad (2.23)$$

which can be put in the form,

$$F_v' (J_r) = B_{\text{eff}} + D_v' [(J_r + 2)(J_r + 5) - 2] J_r (J_r + 1)$$

where $B_{\text{eff}} = \Delta F' / 6 (J_r + 2)$ (2.24)

T_v , the upper state vibrational term values are calculated from the expression

$$T_v = T(J_r) - F_v' (J_r)$$

The experimental $\delta(R_2 P_1)$ in the range $0 \leq v \leq 44$ are used to obtain an average value of $\Delta F'$. On the basis of these calculations, it appears that there are two possible schemes for the upper state (see

table 2.10). 1) All resonance series have originated from the same upper electronic state. Fig. 2.6 shows the upper state levels with T_v values and B_{eff} values. The separation between the levels A_{12} and A_{34} is 68 cm^{-1} and that between A_{12} and G is 468 cm^{-1} . This shows that seven vibrational levels are probably involved with an average vibrational quantum (w) 67 cm^{-1} between these levels. Extending these assignments and calling the vibrational index corresponding to the lowest excited level G as n ,

one has $v' = n+29$ for the highest level E. The vibrational quantum numbers for the levels A_{12} , A_{34} and B come out to be $n + 7$, $n + 8$, and $n + 25$ respectively.

As the B_{eff} and hence T_v values could be obtained for the quartet series alone by the above method, to a first approximation. B_{eff} values of series D and C are assumed to be those of their nearest neighbours i.e., $2.719 \times 10^{-2} \text{ cm}^{-1}$ for D and $2.791 \times 10^{-2} \text{ cm}^{-1}$ for C. Then T_v values for the levels D and C are obtained and the corresponding vibrational assignments are $n + 1$ and $n + 23$ respectively. All these assignments are shown in scheme 1 of fig. 2.6.

The B_{eff} values of levels B and E are larger than those of G or A levels. This is quite unexpected as they should decrease with increasing vibrational index. However, it may be partly because of a perturbation and partly because of the errors involved in B_{eff} values.

2) It is equally possible to have two upper electronic states involved in resonance series. Under this scheme levels G_{12} , D, A_{12} , A_{34} and C belong to one electronic state with $w \sim 67 \text{ cm}^{-1}$ and the vibrational assignments the same as those in scheme one. But series B and E belong to one upper electronic state with four vibrational quanta separating them and $w \sim 61 \text{ cm}^{-1}$. Now all B_{eff} values fall nicely into the frame. The assignments of all these levels are shown under scheme 2 in the fig. 2.6.

The electronic state $^1\overline{\Sigma}^+(0_u^+)$ arising from the configuration $\sigma_g \pi_u^4 \pi_g^4 \sigma_u$ seems to be the upper state under scheme 1. Under scheme 2, $^3\Sigma^-(v_u^+)$ arising from the configuration $\sigma_g^2 \pi_u^3 \pi_g^3 \sigma_u^2$ probably corresponds to G, A₁₂, A₃₄ and D, while $^1\Sigma^+(0_u^+)$ arising from $\sigma_g \pi_u^4 \pi_g^4 \sigma_u$ probably is responsible for B and E.

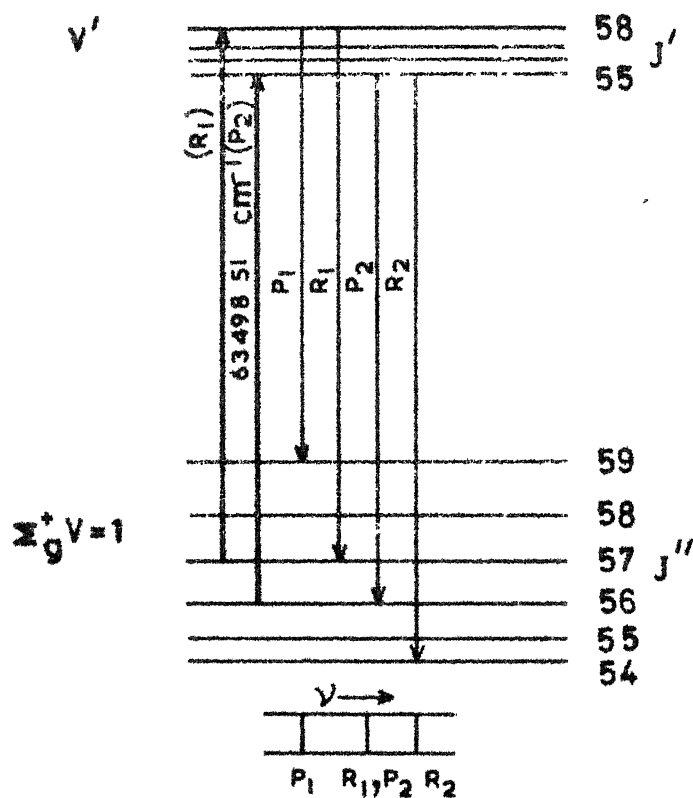
Venkateswarlu has recorded the absorption spectrum of ⁷⁹Br₂, ⁸¹Br₂ in the vacuum ultraviolet covering a region 6300v-66500cm⁻¹ which shows discrete bands. A preliminary analysis shows that ΔG_{v+1} is 65cm⁻¹. A detailed analysis might throw light whether one or two electronic states are involved in this region.

Conclusions

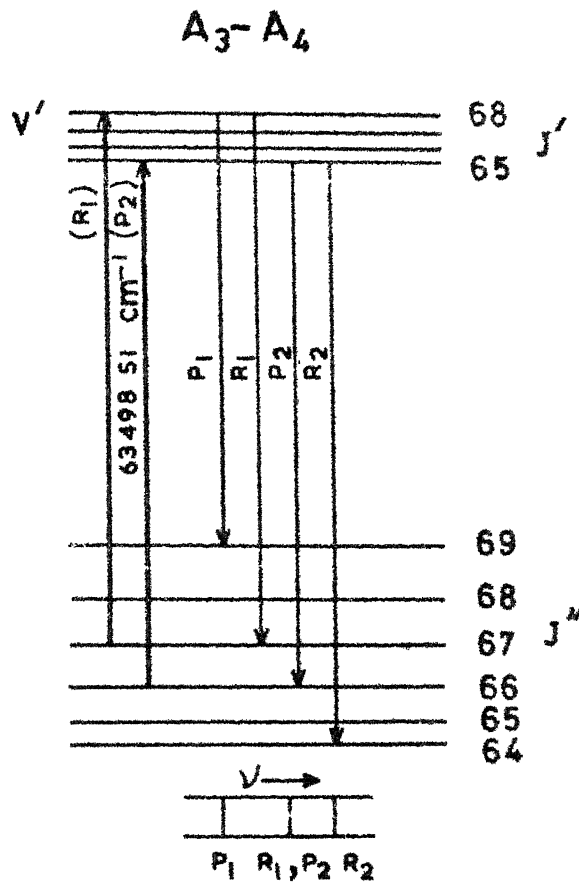
The doublet separations calculated from this work and those calculated from molecular constants of Barrow et al.²⁹ agree well with each other, the differences being 0.03 cm⁻¹. The constants presented here are more meaningful as they are obtained from extensive data while those reported by Barrow et al.²⁹ for ^{79,81}Br₂ are calculated from the work on isotopes ⁷⁹Br₂ and ⁸¹Br₂. Comparison of G_o(v) of this work with those of Barrow et al. upto v = 10 show clearly that there is good agreement which is not unexpected.

$A_1 - A_2$

$A_3 - A_4$



(a)

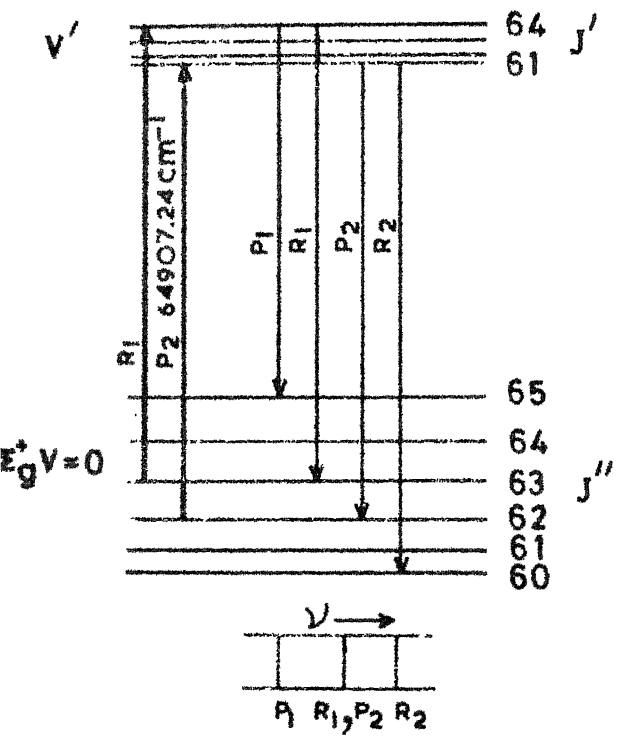


(b)

Fig. 2.1 Excitation process of quartet series (a) $A_1 - A_2$ and (b) $A_3 - A_4$. The resonance lines are shown at the extreme left. The frequency of the resonance line in each case is equal to R_1 (A_1 or A_3) and P_2 (A_2 or A_4). The appearance of triplets is due to the overlap of R_1 and P_2 as shown below the energy level diagrams.

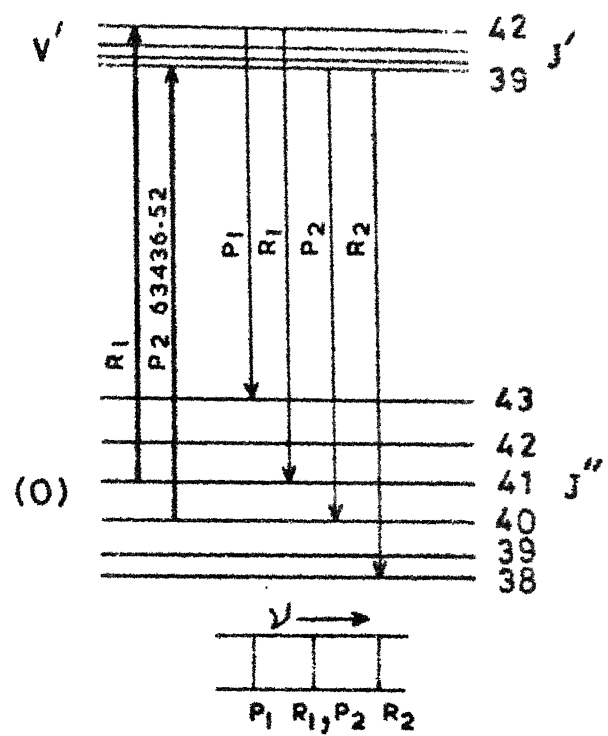
$B_1 - B_2$

(a)



$G_1 - G_2$

(b)



c

→ INCREASING v

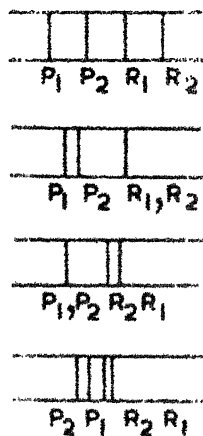


fig. 2.2 Excitation mechanism of quartet series (a) $B_1 - B_2$ and (b) $G_1 - G_2$. The atomic lines, lower and upper state quantum numbers are shown. The general nature of a quartet as increases is shown with the B series as an example.

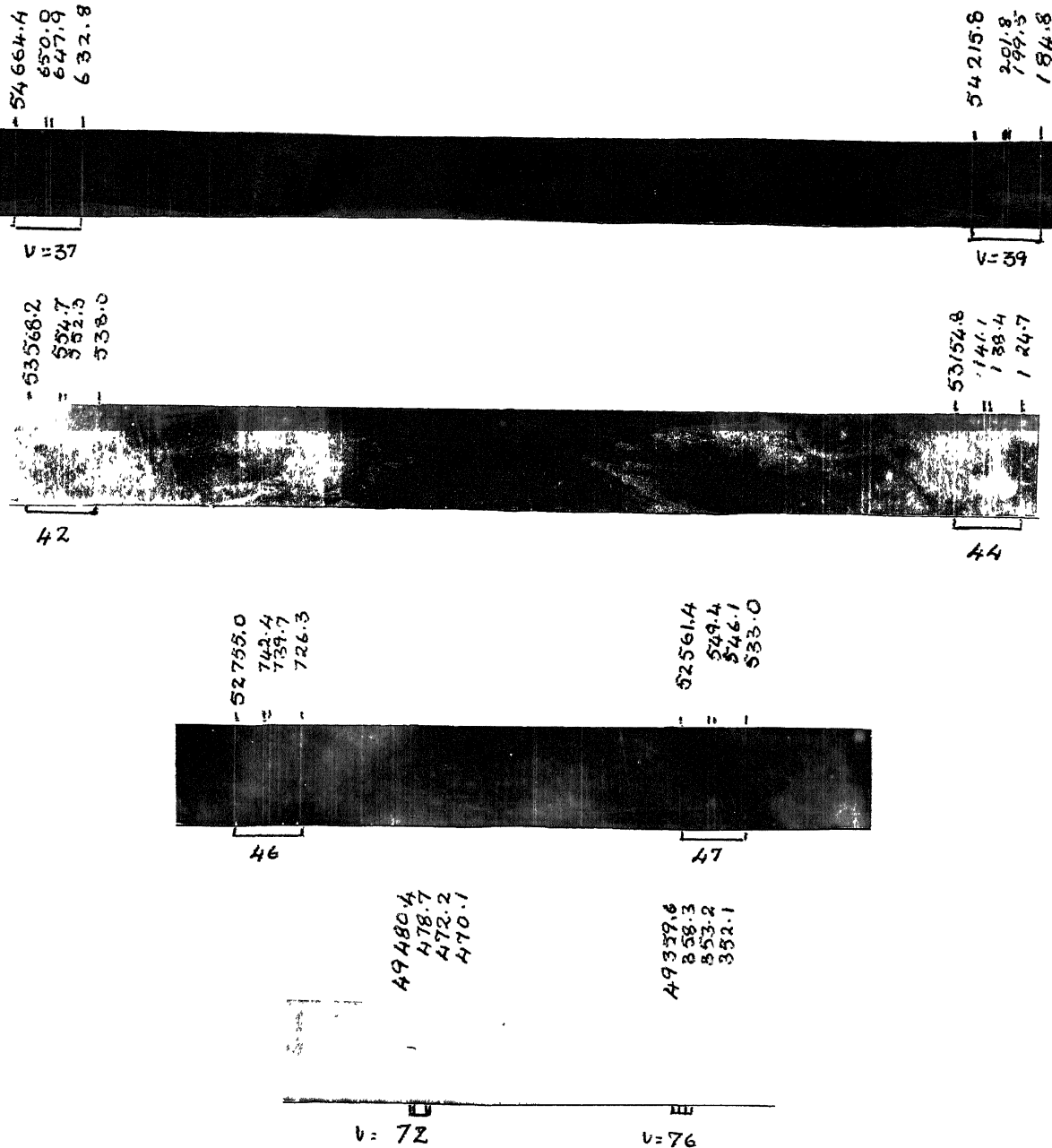


Fig. 2.2b Quartet series B_1 - B_2 . The vibrational assignments and the wave numbers are marked.

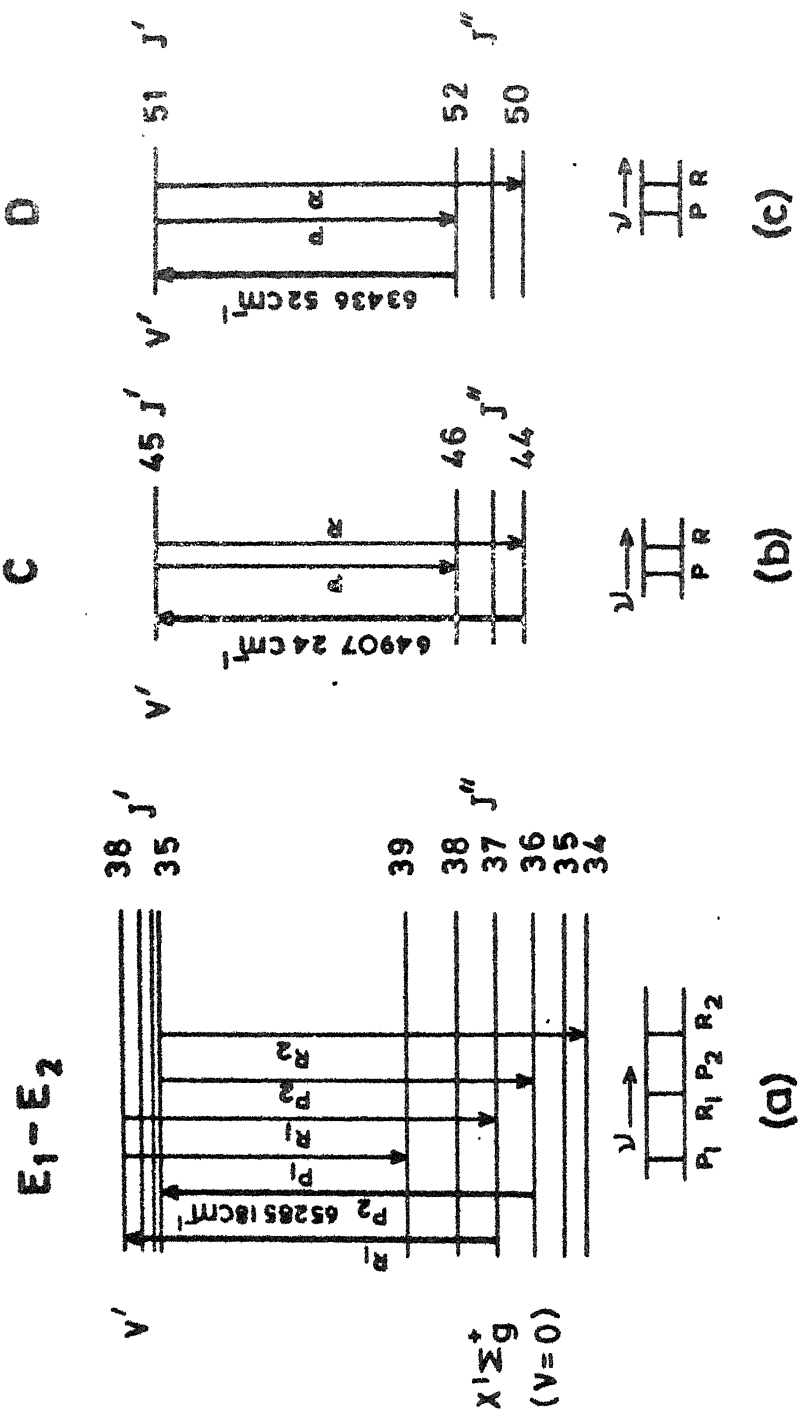


Fig. 2.3 Origin of series (a) $E_1 - E_2$, (b) C and (c) D. The latter two give only doublets. All the quantum numbers are indicated.

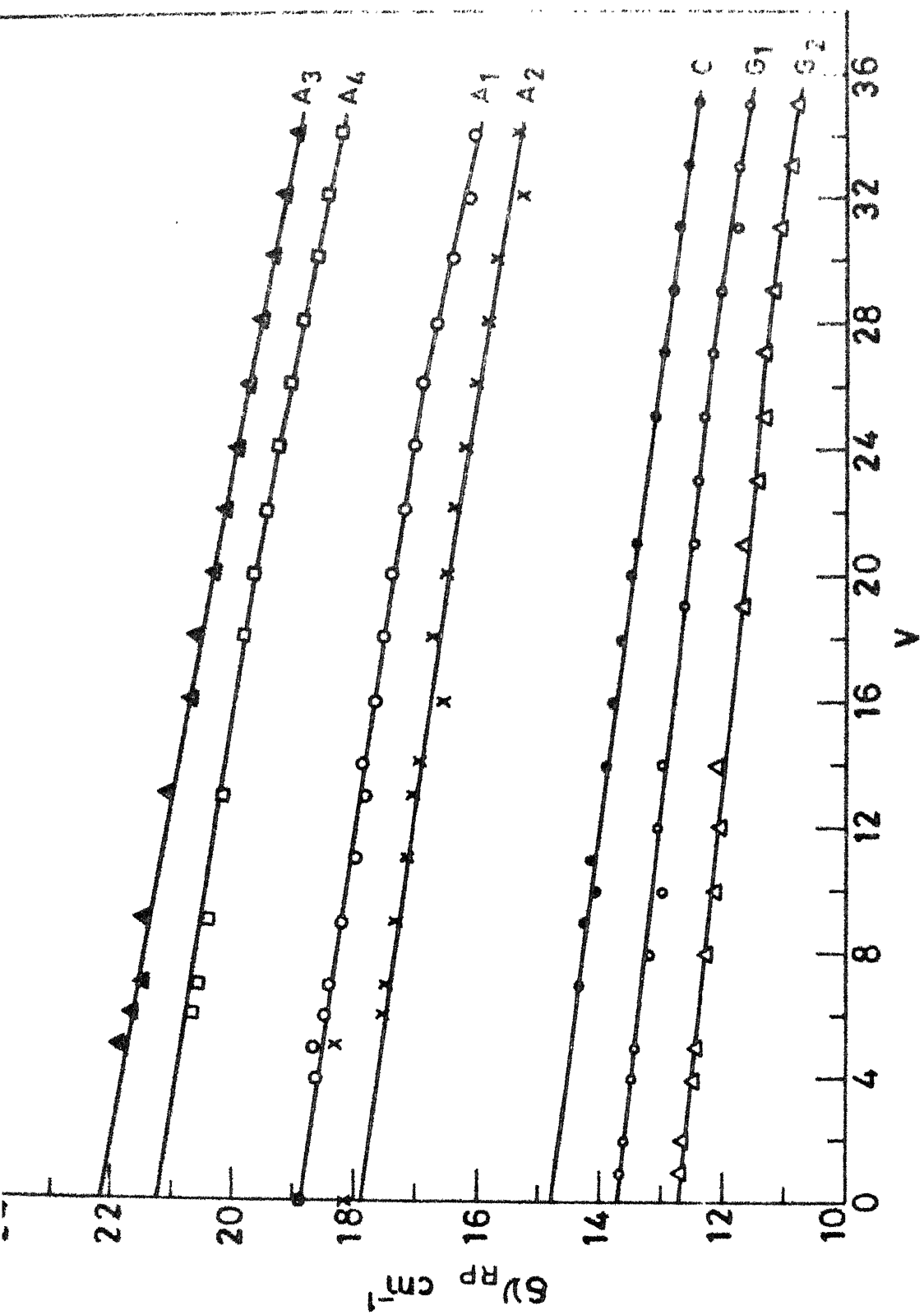


Fig. 2.4 Plots of δD_{RP} against V for the series A_1 , A_2 , A_3 , A_4 , C , G_1 and G_2 . Each of the plots is marked with its name.

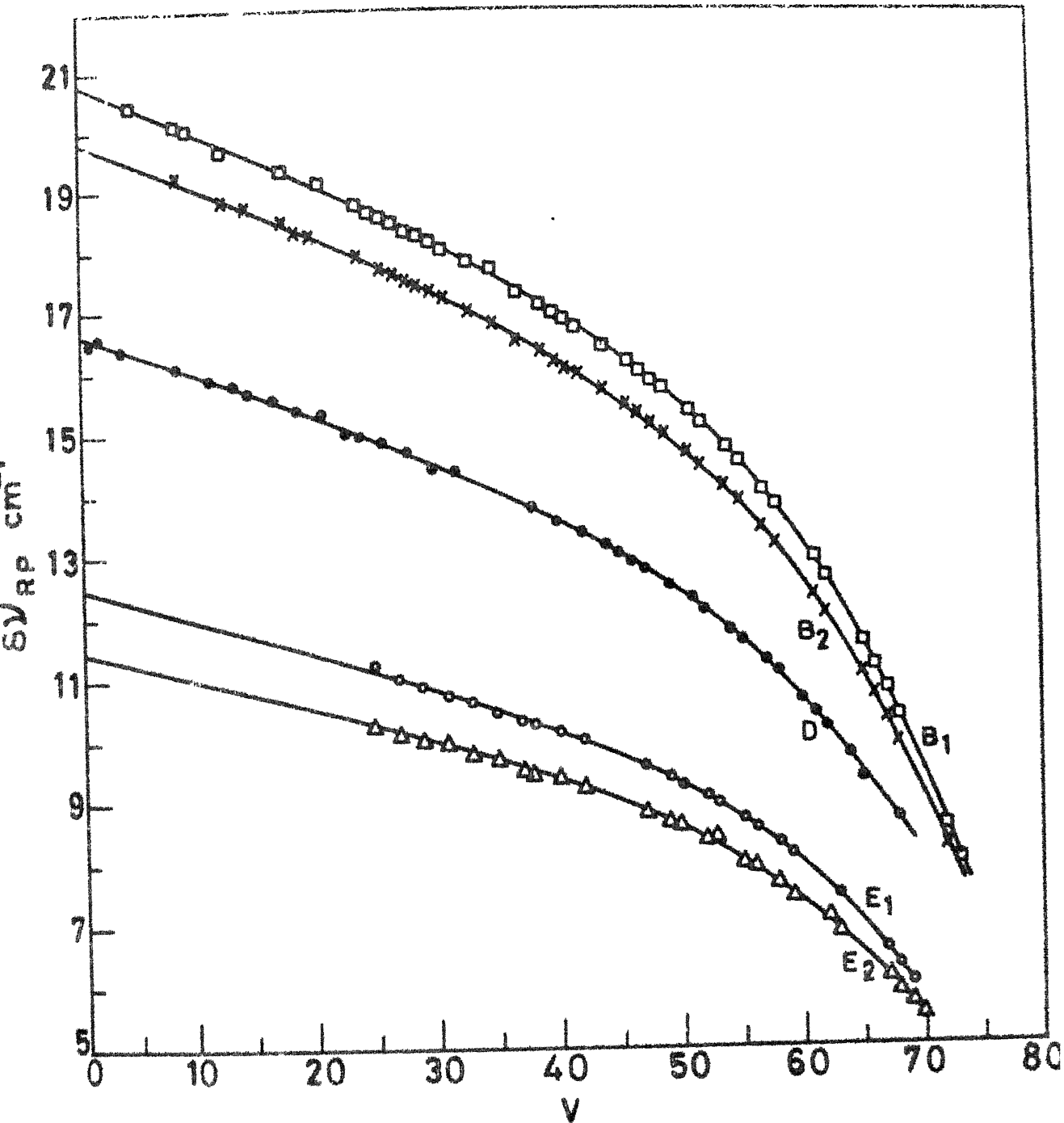


Fig. 2.5 Plots of $\delta\nu_{RP}$ versus v for series B_1 , B_2 , D , E_1 and E_2 .

	$^3\Sigma^-(O_u^+)$	$^1\Sigma^+(O_u^+)$	τ_v	θ_v
Scheme 2				
$n' + 4$	$n + 29$	E		
n'	$n + 25$	B		
$n + 23$	$n + 23$	C		
			65358.76	2.734
			65117.71	2.791
			65010.33	2.791
Scheme 1				
$n' + 4$	$n + 29$	E		
n'	$n + 25$	B		
$n + 23$	$n + 23$	C		
			64064.38	2.612
			63996.29	2.635
			63527.00	2.719

Fig. 2.6 The energy levels and the possible schemes for the upper electronic state/states. The vibrational term values, the rotational constants and the vibrational assignments of the energy levels are indicated.

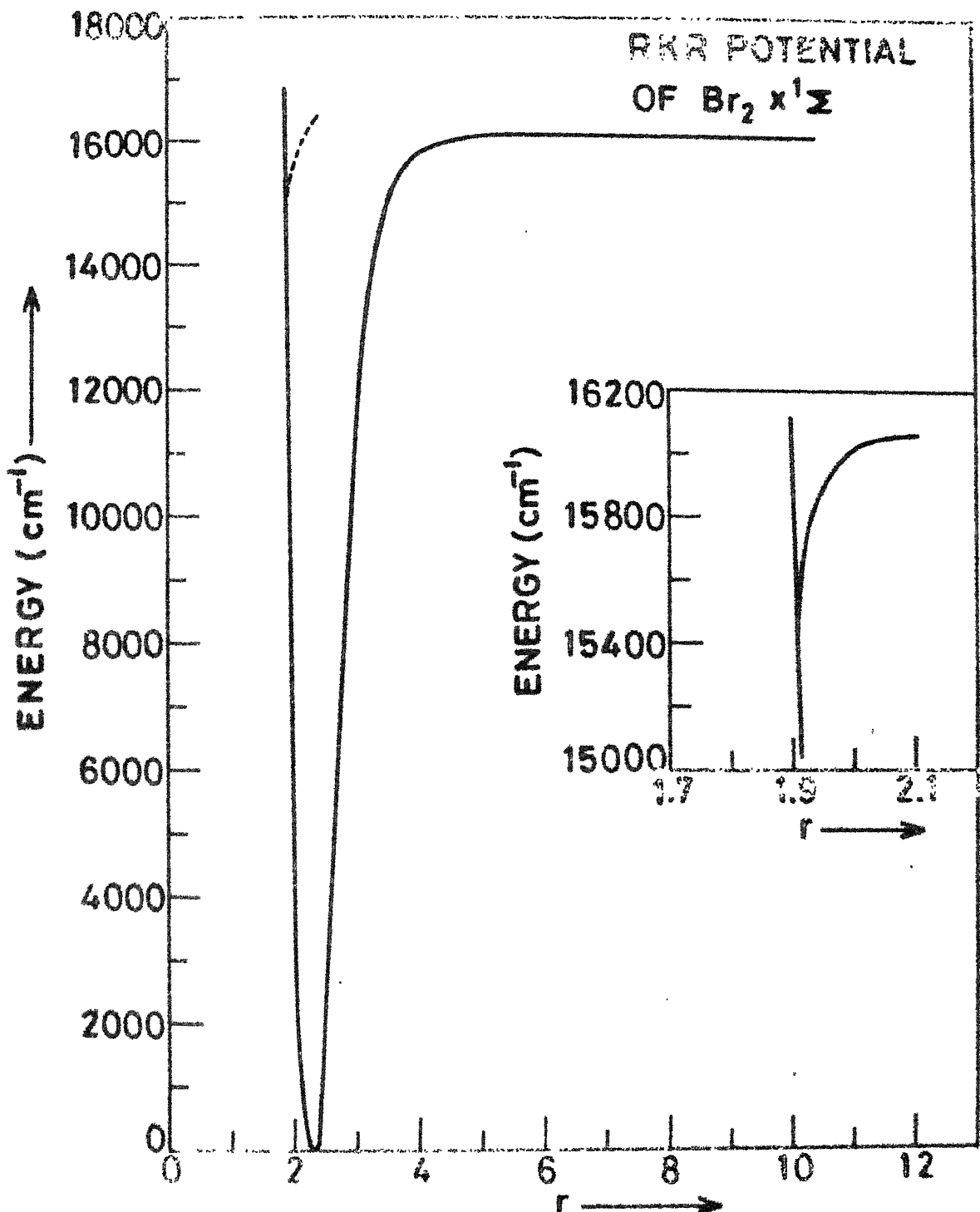


Fig. 2.7 RKR potential of Bromine X state. Above 15000cm^{-1} the potential turns inward as indicated by the dotted line. The irregularity is corrected as described in Chapter 3. The inset shows an enlarged portion of this region.

TABLE 2.1

 A_1, A_2 Doublet Series

v	P ₁	δ	R ₁	P ₂	δ	R ₂
0	63799.75	18.89		63818.64	18.18	63836.82
4	62532.63	13.54		62551.17		
5	62221.1	18.05		62239.75	18.25	62258.0
6	61912.10	13.45		61930.55	17.45	61948.0
7	61605.19	18.35		61623.54	17.41	61640.95
9	60998.05	13.12		61016.17	17.22	61033.39
11	60399.98	17.92		60417.9	17.04	60434.94
13	59811.09	17.71		59828.80	16.93	59845.74
14	59520.22	17.81		59538.03	16.61	59554.64
16	58945.60	17.57		58963.17	16.45	58979.62
18	58380.54	17.55	58397.99	58397.51	16.63	58414.14
20	57825.19	17.31	57842.50	57842.00	16.39	57858.39
22	57279.97	17.00	57297.05	57296.42	16.32	57312.74
24	56744.88	16.98	56761.86	56761.16	16.08	56777.24
26	56220.32	16.80	56237.12	56236.32	15.93	56252.25
28	55706.47	16.61	55723.03	55722.19	15.78	55737.97
30	55203.66	16.33	55219.99	55219.04	15.56	55234.60
32	54712.05	16.01	54723.06	54727.32	15.19	54742.51
34	54232.33					54262.03

N.B : all the doublets are in cm^{-1} .

TABLE 2.2

 A_3, A_4 Doublet Series

v	P ₁	$\delta\nu$	R ₁	P ₂	$\delta\nu$	R ₂
0	63796.22	22.42		63818.64	21.07	63839.71
1				63498.51		
5	62219.63	21.84		62241.47	21.49	62262.96
6				61932.59	20.63	61953.22
7	61604.63	21.40		61626.05	20.50	61646.53
9	60998.05	21.43		61019.48	20.31	61039.79
13	59812.76	20.94		59833.70	20.07	59853.77
16	58949.00	20.60	58969.60	58969.10	19.73	58988.83
18	58384.71	20.54	58405.25	58404.66	19.60	58424.26
20	57830.41	20.25	57850.66	57849.92	19.40	57869.32
22	57286.03	20.03	57306.11	57305.31	19.16	57324.47
24	56752.04	19.35	56771.89	56770.94	19.02	56789.96
26	56228.43	19.66	56248.09	56247.06	18.77	56265.83
28	55715.61	19.45	55735.06	55733.89	18.54	55752.43
30	55213.78	19.23	55233.01	55231.73	18.37	55250.10
32	54723.45	19.06	54742.51	54741.02	18.19	54759.21
34	54244.64	18.84	54263.48	54262.05	17.97	54279.96
36	53778.20	13.47	53790.67	53795.05	17.62	53812.67

N.B. . All the doublets are in cm^{-1} .

TABLE 2.3

 G_1, G_2 Doublet series

v	P_1	c	R_1	ν_2	$\delta\nu$	μ_2
0				63436.52		
1	63102.03	13.70	63115.73	12.68	63128.41	
2	62783.59	13.62	62797.21	12.65	62809.86	
4	62153.35	13.47	62166.82	12.43	62179.30	
5	61841.46	13.43	61854.89	12.48	61867.30	
8	60919.10	13.17	60932.27	12.25	60944.51	
10	60315.35	12.98	60328.31	12.10	60340.41	
12	59720.71	13.06	59733.77	12.09	59745.61	
14	59135.52	13.00	59148.52	12.12	59160.22	
19	57714.01	12.62	57726.69	11.64	57737.3	
21	57162.49	12.50	57174.99	11.66	57186.10	
23	56621.06	12.41	56633.47	11.43	56644.28	
25	56089.54	12.35	56102.27	11.52	56112.95	
27	55569.41	12.14	55581.55	11.31	55592.05	
29	55059.73	12.03	55071.76	11.15	55082.04	
31	54561.21	11.77	54572.98	11.09	54583.21	
33	54074.09	11.75	54085.84	10.32	54095.74	
35	53598.90	11.50	53610.40	10.70	53620.15	

N.B. . All the doublets are in cm^{-1} .

TABLE 2.4

 E_1, E_2 Doublet Series

v	P_1	δv	R_1	P_2	δv	R_2
65285.18						
25	57937.25	11.25	57948.50	57947.33	10.24	57953.07
27	57416.53	11.01	57427.54	57426.83	10.11	57436.94
29	56906.60	10.87	56917.47	56916.69	10.02	56926.71
31	56407.82	10.74	56418.56	56417.60	9.93	56427.58
33	55920.40	10.61	55931.01	55930.17	9.75	55939.92
35	55444.90	10.40	55455.30	55454.30	9.71	55464.01
37	54981.60	10.30	54991.90	54990.89	9.49	55000.38
38	54749.7	10.25	54764.96	54763.92	9.46	54773.38
40	54310.69	10.13	54320.82	54319.6	9.42	54329.02
42	53880.15	10.01	53890.16	53883.93	9.20	53898.13
47	52867.60	9.56	52877.16	52875.71	8.83	52884.54
49	52490.06	9.37	52499.43	52497.3	8.69	52506.49
50	52307.68	9.26	52316.94	52315.27	8.65	52323.92
52	51956.37	9.04	51965.41	51963.75	8.35	51972.08
53	51787.75	8.93	51796.73	51794.34	8.38	51803.22
55	51465.54	8.65	51474.20	51472.57	8.0	51480.37
56	51312.29	8.58	51320.87	51313.97	7.90	51326.87
58	51022.55	8.26	51030.81	51028.77	7.01	51036.38
59	50886.47	8.12	50894.59	50892.54	7.43	50899.97
62	50516.09	7.81	50523.9	50521.3	7.10	50528.40
63	50405.93	7.42	50413.35	50410.90	6.84	50417.74
67	50035.40	6.56	50041.96	50030.09	5.10	50045.19
68	49960.43	6.27	49966.70	49963.73	5.38	49969.66
69	49892.49	6.0	49898.49	49895.39	5.67	49901.06

N.B. All the doublets are in cm^{-1} .

TABLE 2.5

 B_1, B_2 Doublet Series

v	P ₁	$\delta\tau$	R ₁	P ₂	$\delta\tau$	R ₂
0				64907.24		
9	62087.10	20.10	62107.20	62106.50	19.20	62125.70
13	60901.40	19.65	60921.05	60920.00	18.78	60938.87
18	59471.99	19.30	59491.29	59490.05	18.41	59508.46
19	59193.43	19.37	59212.80	59211.45	18.23	59229.68
20	58917.25	19.22	58936.47	58935.15	18.20	58953.33
21	58643.67	19.10	58662.77	58661.31	17.95	58679.26
24	57838.02	18.75	57856.75	57855.26	17.83	57873.14
25	57574.68	18.61	57593.29	57591.83	17.73	57609.56
26	57314.01	18.51	57332.52	57330.95	17.65	57348.60
27.	57056.03	18.45	57074.48	57072.33	17.50	57090.38
28	56800.81	18.28	56819.09	56817.42	17.45	56834.37
29	56543.29	18.22	56566.51	56564.76	17.36	56582.12
30	56293.56	18.13	56316.69	56314.33	17.30	56332.18
31	56051.69	17.98	56069.67	56067.84	17.16	56085.00
33	55566.57	17.78	55584.35	55582.43	16.95	55599.33
35	55093.45	17.50	55111.01	55108.96	16.74	55125.70
37	54632.76	17.23	54650.04	54647.33	16.49	54674.37
39	54184.81	17.03	54201.34	54199.54	16.30	54215.34
40	53965.71	16.94	53982.05	53980.32	16.13	53996.45
41	53750.11	16.85	53760.96	53764.54	16.00	53780.54
42	53538.03	16.70	53554.73	53552.25	15.91	53568.16
44	53124.66	16.39	53141.05	53138.42	15.66	53154.08
46	52726.29	16.13	52742.12	52730.55	15.35	52755.00
47	52533.05	15.97	52549.02	52546.15	15.24	52561.39

TABLE 2.5 (Continued)

v	P ₁	δv	R ₁	P ₂	δv	R ₂
48	52343.84	15.80	52359.64	52356.70	15.02	52371.72
49	52158.97	15.59	52174.56	52171.58	14.39	52186.47
51	51302.26	15.33	51317.59	51314.40	14.59	51328.99
52	51630.89	15.10	51645.99	51642.75	14.37	51657.12
54	51302.30	14.70	51317.50	51314.05	14.05	51328.10
55	51146.46	14.49	51160.95	51157.38	13.81	51171.19
57	50850.34	14.00	50864.34	50860.57	13.37	50873.94
58	50710.89	13.78	50724.67	50720.73	13.14	50733.92
61	50330.16	12.95	50343.11	50338.83	12.28	50351.11
62	50216.46	12.60	50229.06	50224.64	11.93	50236.62
65	49917.69	11.56	49929.25	49924.32	11.05	49935.37
66	49832.60	11.19	49845.79	49833.64	10.68	49849.32
67	49754.79	10.79	49765.58	49760.22	10.31	49770.53
68	49684.16	10.39	49694.55	49680.98	9.91	49698.89
72	49470.12	8.55	49478.67	49472.18	8.12	49480.40
73	49432.40	8.10	49440.50	49435.77	7.76	49441.53
76	49353.21	6.40	49359.61	49352.14	6.12	49358.26

TABLE 2.6A
U Doublet series

V	P	R	δv
0		64907.24	
5	63312.05	63326.88	14.83
6	63002.66	63017.20	14.54
7	62695.04	62709.37	14.33
9	62087.11	62101.37	14.26
10	61736.60	61800.67	14.07
11	61438.20	61502.33	14.13
13	60898.50	65911.74	13.24
14	60607.04	60620.92	13.36
16	60031.33	60045.12	13.79
18	59465.33	59478.98	13.65
20	58909.09	58922.57	13.48
21	53654.72	53643.10	13.38
24	57825.19	57833.02	12.83
25	57562.51	57575.59	13.08
27	57042.20	57055.18	12.94
29	56522.73	56545.52	12.79
31	56034.57	56047.07	12.70
33	55547.47	55560.09	12.50
35	55072.52	55084.38	12.36

TABLE 2.6B
D Doublet Series

v	P	R	$\delta\tau$	v	P	R	$\delta\tau'$
0	63456.52			40	52492.27	52505.30	13.53
1	63116.18	63132.67	16.49	42	52063.02	52076.53	13.36
2	62797.95	62814.49	16.54	44	51647.93	51661.07	13.14
4	62168.30	62184.70	16.40	45	51445.97	51458.98	13.01
9	60632.39	60648.46	16.07	46	51247.83	51260.72	12.89
12	59737.89	59753.77	15.86	47	51053.64	51066.42	12.73
14	59153.32	59159.06	15.74	49	50677.67	50690.17	12.50
15	58864.51	58880.16	15.05	51	50513.97	50531.25	12.28
17	58294.07	58309.60	15.53	52	50146.47	50153.57	12.10
19	57733.28	57743.64	15.36	54	49616.06	49627.79	11.73
21	57132.33	57197.63	15.30	55	49653.45	49670.08	11.63
23	56641.66	56656.62	14.96	57	49359.55	49370.80	11.27
24	56375.17	56390.09	14.92	58	49213.70	49229.80	11.10
26	55349.95	55364.75	14.80	60	48955.17	48955.79	10.62
28	55335.43	55350.11	14.63	61	48833.00	48843.38	10.38
30	54832.05	54848.44	14.39	62	48717.57	48727.77	10.20
32	54339.87	54354.22	14.35	64	48507.06	48516.68	9.62
38	52935.14	52943.90	13.76	65	48412.49	48421.82	9.33

TABLE 2.7

Frequencies and Quantum Numbers of the Exciting Lines

Series	Exciting line	a_0	$J' = J_r$	V	J''	Δ
A ₁	63498.51	18.76	58	1	57	0.0
A ₂	63498.51	17.80	55	1	56	0.0
A ₃	63498.51	21.99	68	1	67	-0.12
A ₄	63498.51	20.99	65	1	66	-0.16
B ₁	64907.24	20.89	64	0	63	0.25
B ₂	64907.24	19.94	61	0	62	0.28
C	64907.24	14.69	45	0	44	-0.13
D	63436.52	16.58	51	0	52	-0.09
E ₁	65285.18	12.48	38	0	37	0.28
E ₂	65285.18	11.50	35	0	36	0.25
G ₁	63436.52	13.73	42	0	41	0.21
G ₂	63436.52	12.68	39	0	40	0.24

[†] Exciting line and a_0 are in cm^{-1} .

1977 Dec 6 0

MAGNETIC FIELD DATA FOR 1977 DEC 6 (A=STATS)

THE FOLLOWING TABLE GIVES THE MAGNETIC FIELD DATA FOR 1977 DEC 6.

	1.0	4	82
1	1.000+2.8	2.023+1.2	2.033+3.3
2	2.000+0.1	2.033+1.0	2.037+3.1
3	3.000+3.9	2.017+7.0	2.040+7.0
4	4.000+1.8	2.015+9.1	2.043+2.9
5	4.033+1.2	2.013+1.2	2.045+5.2
6	4.063+2.0	2.012+3.0	2.047+2.3
7	2.055+8.9	2.011+9.3	2.049+1.2
8	2.053+2.9	2.010+8.7	2.051+3.2
9	2.054+7.2	2.009+9.1	2.053+1.5
10	2.073+3.3	2.009+1.6	2.054+5.0
11	3.073+6.5	2.006+2.6	2.056+2.6
12	3.073+7.3	2.007+9.0	2.058+1.0
13	3.073+5.1	2.005+7.5	2.059+1.8
14	3.055+3.1	2.005+1.0	2.061+3.0
15	3.057+1.0	2.005+5.7	2.062+3.4
16	3.059+2.7	2.002+8.7	2.064+4.7
17	3.053+4.1	2.004+3.3	2.065+0.7
18	3.053+4.7	2.004+7.0	2.067+2.2

V	G(V)	R1	R2
19	5602.10	2.03241	2.69026
20	5882.29	2.02743	2.70520
21	6160.02	2.02265	2.72007
22	6435.25	2.01896	2.73487
23	6707.96	2.01362	2.74953
24	6978.11	2.00934	2.76436
25	7245.59	2.00520	2.77906
26	7510.65	2.00118	2.79375
27	7772.97	1.99729	2.80847
28	8032.62	1.99350	2.82320
29	8289.55	1.98982	2.83795
30	8543.74	1.98623	2.85276
31	8795.15	1.98274	2.86762
32	9043.74	1.97933	2.88256
33	9289.47	1.97601	2.89758
34	9532.29	1.97276	2.91271
35	9772.17	1.96959	2.92795
36	10009.05	1.95650	2.94334
37	10242.88	1.95348	2.95887
38	10473.61	1.95054	2.97458
39	10701.18	1.95766	2.99049
40	10925.53	1.95486	3.00561
	11146.59	1.95213	3.02297

	S(V)	R1	R2
51	11384.30	1.94948	3.03981
52	11578.58	1.94690	3.05554
53	11789.36	1.94439	3.07379
54	11996.53	1.94197	3.09141
55	12200.02	1.93982	3.10943
56	12399.72	1.93736	3.12799
57	12595.54	1.93518	3.14685
58	12787.35	1.93308	3.16534
59	12975.04	1.93108	3.18642
50	13158.17	1.92916	3.20715
51	13337.51	1.92734	3.22862
52	13512.02	1.92561	3.25088
53	13681.82	1.92397	3.27404
54	13846.76	1.92243	3.29820
55	14006.66	1.92098	3.32346
56	14161.32	1.91963	3.34997
57	14310.53	1.91836	3.37787
58	14454.08	1.91718	3.40735
59	14591.74	1.91606	3.43862
60	14723.26	1.91501	3.47193

TABLE 2.9

Molecular Constants of $^{79,81}\text{Br}_2$ (cm^{-1})⁺

Preliminary Rotational Constants:

$$B_e = 8.1129 \times 10^{-2}, \quad \alpha_e = 2.9428 \times 10^{-4}, \quad \gamma_e = -1.599 \times 10^{-6}; \\ D_e = 3.7089 \times 10^{-8}, \quad \beta_e = 1.434 \times 10^{-9};$$

for the range $0 \leq v \leq 36$

Final Rotational Constants:

$$B_e = 8.0911 \times 10^{-2}, \quad \alpha_e = 2.1397 \times 10^{-4}, \quad \gamma_e = -9.1929 \times 10^{-6}, \\ \delta_e = 2.5419 \times 10^{-7}, \quad \varphi_e = -2.8324 \times 10^{-9}; \\ D_e = 3.3389 \times 10^{-8}, \quad \beta_e = 1.614 \times 10^{-9},$$

for the range $0 \leq v \leq 70$

Vibrational Constants:

$$C_1 = 3.2343 \times 10^2, \quad C_2 = -1.1013, \quad C_3 = 1.6061 \times 10^{-3}, \\ C_4 = -1.6759 \times 10^{-4}, \quad C_5 = 2.8169 \times 10^{-6}, \\ C_6 = -2.4609 \times 10^{-8},$$

for the range $0 \leq v \leq 60$

$$w_e = 323.34, \quad w_e x_e = 1.0758, \quad w_e y_e = -1.0252 \times 10^{-4} \\ g(0) = 161.405$$

⁺ All the constants are in cm^{-1} .

TABLE 2.10

Rotational Constants and Energy levels of the Upper state

Series	$10^2 \times \nu_{\text{eff}}$	$F'(J_r)$	$E(J_r)$	E_v	v'	
					11	2
G ₁	2.719	49.16	63576.09	63526.98	n	n
G ₂		42.42	63569.44	63527.27		
D	(2.719)	172.11	63659.73	63587.62	n+1	n+1
A ₁	2.635	90.15	64086.42	63996.31	n+7	n+7
A ₂		81.14	64077.45	63996.27		
A ₃	2.612	122.55	64186.96	64064.35	n+3	n+8
A ₄		112.05	64176.40	64064.41		
C	(2.791)	57.77	65068.10	65117.64	n+23	n+23
B ₁	2.791	116.11	65233.89	65117.64	n+25	n'
B ₂		105.56	65223.32	65117.78		
E ₁	2.734	40.52	65399.27	65358.75	n+29	n'+4
E ₂		34.45	65393.21	65358.76		

CHAPTER 3

LONG-RANGE ANALYSIS OF THE X AND B STATES OF Br₂

Introduction

The wealth of the results presented in the second chapter was best utilised in obtaining the long-range molecular constants of Br₂ $\Delta \sum_g^+$ state for the first time. The results of the analysis were quite rewarding. The asymptotic value of the power n, in the inverse power series expansion of the potential is shown to be 6, for the ground state of bromine. This knowledge was used in extrapolating vibrational spacings and rotational constants upto the dissociation limit. The correct potential was obtained from this data using the methods described in chapter 1. Long-range analysis of the outer turning points was carried out to obtain inverse-power potential coefficients, C₆ and C₈. Similarly using the data of Barrow et al.,²⁹ long-range molecular constants of the B state of bromine were obtained.

The Long-range Analysis of X State : ^{79,81}Br₂

The Birge-Spooner plot (fig. 4.1) of the vibrational energy levels in the range 60 ≤ v ≤ 76, shows a positive curvature above v = 65 as expected¹⁰ for a potential of the form

$$V(r) = D - \sum_m C_m / r^m \quad (3.1)$$

When all the leading terms in this equation have the same sign, it may be approximated in any interval of the long-range region by

$$V(r) = D - C_n / r^n \quad (3.2)$$

where C_n / r^n is the effective single term for the whole of the interval.

A theoretical value of $n = 6$ was suggested by Le Roy and Bernstein.¹⁰ However, the experimental determination of the value of n is an essential first step in the long-range analysis. Towards this end the dissociation energy, D was determined from least squares fit of the vibrational energies, $G(v)$ as a function of ΔG_v to the eq. 3.3 (for several values of n from 4.5 to 7.5). The points in the range $72 = v = 76$ were used in the fits and the results given in table 3.1. (Fig. 3.1).

$$G(v) = D - K (\Delta G_v)^{2n/(n+2)} \quad (3.3)$$

Since the standard deviations of these fits are relatively insensitive to variations in n , it is sought to fix n on the basis of the agreement of value of D with the known value. Now as the value of n varies from 4.5 to 6,

* D , the dissociation energy should not be confused with series D of chapter 2.

D decreases from 15914.54cm^{-1} to 15897.03cm^{-1} (table 3.1).

As explained in the first chapter, the value of D obtained from each of the above fits is an upper bound. Hence, the value of n is fixed as 6, which agrees with the theoretical value. Substituting this value of n in eqs. 1.23, 1.24 and rearranging the terms, the following two equations are obtained.

$$[D - G(v)]^{1/3} = H_6 (v_D - v) \quad (3.4)$$

$$B_v = \omega_6 (v_D - v) \quad (3.5)$$

Using the known value of $D = 15895.63\text{cm}^{-1}$, eq. 3.4 was fitted by linear regression over the range $71 \leq v \leq 76$ and $H_6 = 0.3347$, $v_D = 88.94$ were obtained. Vibrational energies, $\epsilon(v)$ were then extrapolated from $v = 76$ upto the dissociation limit ($v_D = 89$). Adopting similar procedures, B_v values beyond $v = 76$ were extrapolated using eq. 3.5 where $\omega_6 = 0.1981$ and $v_D = 89.01$. The B_v and $G(v)$ values were included in table 3.2. The values of C_6 calculated from H_6 and ω_6 are respectively, $3.042 \times 10^5 \text{cm}^{-1} \text{A}^6$ and $11.95 \times 10^5 \text{cm}^{-1} \text{A}^6$. The latter is very large as expected because eq. 3.5 is less accurate than eq. 3.4.⁴

The extrapolated values of $G(v)$ and B_v were used to extend the potential beyond $v = 76$. The RKR method of calculating the turning points at very high vibrational levels is inaccurate as explained in the first chapter.

Hence, using the extrapolated vibrational energies the widths, $[r_2 - r_1]$ computed by a fortran programme, were added to the r_1 values calculated from the relation

$$V(r_1) = a/r_1^{12} + b \quad (3.6)$$

The constants $a = 4.5043 \times 10^7 \text{ cm}^{-1} \text{ \AA}^{12}$ and $b = 3.3755 \times 10^3 \text{ cm}^{-1}$ are determined by least squares fit of $G(v)$ and the r_1 values in the range $50 \leq v \leq 60$ to eq. 3.6. The difference in the r_1 values calculated from eq. 3.6 and the RKR programme, for the highest observed vibrational level $v = 76$, is 0.0119\AA , which shows that the errors introduced by this extrapolation above $v = 60$ are negligible.

The dispersion force constants in eq. 3.1 are determined from the following equations (1.30 and 1.31)

$$[r^6 (D-G(v))]^{-\alpha} = C_6^{-\alpha} - [\alpha C_8 / C_6^{(1+\alpha)}] / r^2, \text{ for } \alpha \neq 0 \quad (3.7)$$

$$\log [r (D-G(v))] = \log C_6 + (C_8 / C_6) / r^2, \text{ for } \alpha = 0 \quad (3.8)$$

In eqs. 3.7 and 3.8, the contributions from higher terms (C_{10} , C_{12} etc.) are effectively represented by the parameter α . The constants C_6 and C_8 were determined from least squares fits of r_2 values for $77 \leq v \leq 87$ to eqs. 3.7 and 3.8 over the range $\alpha = -1.4$ to -0.2 varied in steps of 0.2. The results are given in table 3.3. It is seen from the table, that the minimum RMSD occurs for $\alpha = -0.8$.

The long-range analysis of the same turning points was also performed by fitting them directly to the

linear three-term version of eq. 3.1 (vide eq.1.33)

$$R^5 [D - G(v)] = C_{10} + C_8 R + C_6 R^2 \quad (3.9)$$

Here $R = r^2$, the square of the internuclear distance.

The value of α is calculated from these constants using the relation

$$\alpha = 2(C_{10}C_6/C_8^2) - 1 \quad (3.10)$$

Holding D fixed at the known value of 15895.63cm^{-1} , C_6 , C_8 and C_{10} are determined from the least squares fit of the turning points to the above equation. C_{10} turned out to be negative giving a value of $\alpha = -1.1$, which indicates that $C_{10} = 0$ agreeing with the above conclusion. The constants C_6 and C_8 were determined holding $C_{10} = 0$, and are $3.59 \times 10^5\text{cm}^{-1}\text{\AA}^6$ and $173 \times 10^5\text{cm}^{-1}\text{\AA}^8$ respectively. These are in good agreement with those corresponding to $\alpha = -0.8$ in table 3.3.

$B^3\Pi^- (v_u^+)$ of $^{79}\text{Br}_2$

The attractive part of the KKr potential of the B state of $^{79}\text{Br}_2$ outside the electron-overlap region was investigated on the same lines as those adopted in the study of X state of Br_2 . Yee and Stone⁴³ using the same data, recently obtained dissociation energy and interaction constants C_6 and C_8 . However, they used the theoretical value $1.98 \times 10^5\text{cm}^{-1}\text{\AA}^5$ for C_5 instead of the value determined from the long-range analysis of the

vibrational energies.

In the present work, the experimental values $D = 3339.6 \text{ cm}^l$ and $C_5 = 1.818 \times 10^5 \text{ cm}^{-1} \text{ A}^5$ taken from Barrow et al.²⁹ were used. The results obtained from least squares fits of the turning points for $39 \leq v \leq 52$ to the equations (vide eqs.1.30 and 1.31)

$$[r^6 (D - G(v) - C_5 / r^5)]^{-\alpha} = C_6^{-\alpha} - [\alpha C_8 / C_6]^{(1+\alpha)} / r^2 \quad (3.11)$$

$$\text{and } \log [r^6 (D - G(v) - C_5 / r^5)] = \log(C_6) + (C_8 / C_6) / r^2 \quad (3.12)$$

respectively for the cases where $\alpha \neq 0$ and $\alpha = 0$, are given in table 3.4. The constants obtained from direct fits to four-term equation including C_5 in the right hand side of eq. 3.9, by least squares are $C_6 = 8.54 \times 10^5 \text{ cm}^{-1} \text{ A}^6$, $C_8 = 80.5 \times 10^5 \text{ cm}^{-1} \text{ A}^8$ and $C_{10} = 822 \times 10^5 \text{ cm}^{-1} \text{ A}^{10}$. Although the C_6 values obtained from the two procedures agree well with each other, C_8 values differ markedly.

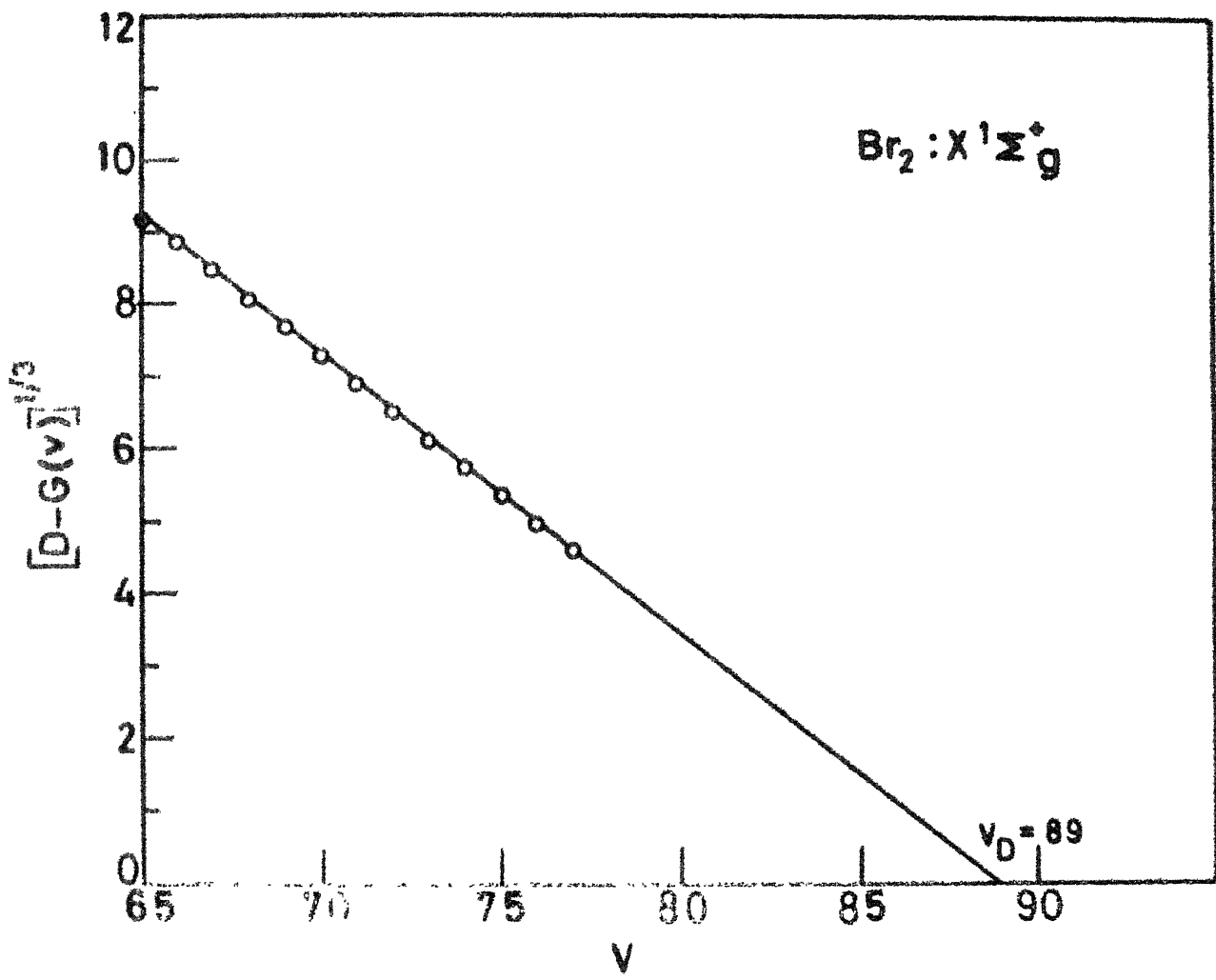


Fig. 3.1 Plot of $[D - G(v)]^{1/3}$ against v near dissociation limit for the X state of Br_2 , which is linear for the range of levels plotted in the graphs. Intercept on the x-axis gives $v_D = 89$, the vibrational index corresponding to dissociation. $[D - G(v)]$ are in cm^{-1} .

TABLE 3.1

n	SD	Dissociation Energy
4.5	0.19	15914.54
5.0	0.16	15907.54
5.5	0.19	15901.81
6.0	0.25	15897.03
6.5	0.32	15892.99
7.0	0.37	15889.53
7.5	0.43	15886.53

Note : SD is the standard deviation of the fit. SD and dissociation energy are in cm^{-1}

TABLE 3.2
SOME COMPUTED POINTS OF PROBABILITY(Y=STATE)

	50% Y=0	30% Y=1	21% Y=2	R2
51	15219.57	0.051090	1.91375	3.50590
52	14967.39	0.050975	1.91274	3.54490
53	15379.47	0.049705	1.91179	3.53570
54	15134.67	0.048476	1.91071	3.52980
55	15282.91	0.047187	1.91009	3.57770
56	15374.15	0.045833	1.90933	3.72950
57	15458.43	0.044413	1.90863	3.78590
58	15535.81	0.042922	1.90799	3.84730
59	15606.44	0.041359	1.90741	3.91430
60	15670.51	0.039719	1.90689	3.98760
61	15728.14	0.038000	1.90642	4.05870
62	15780.11	0.036319	1.90600	4.15340
63	15826.30	0.034310	1.90563	4.25290
64	15867.04	0.032332	1.90530	4.35760
65	15902.67	0.030261	1.90501	4.47570
66	15933.55	0.028169	1.90476	4.60930
67	15960.68	0.026160	1.90455	4.75920
68	15982.37	0.024150	1.90437	4.92900

	R1	R2	R3	R4
7.0	16.231.27	0.022140	1.90422	5.12460
8.0	16.216.23	0.020130	1.90410	5.35240
9.0	16.208.42	0.018120	1.90400	5.62110
10.0	16.207.86	0.016110	1.90392	5.94980
11.0	16.204.98	0.014100	1.90387	6.35230
12.0	16.200.05	0.012090	1.90383	6.87880
13.0	16.203.43	0.010081	1.90380	7.59050
14.0	16.205.46	0.008071	1.90378	8.64630
15.0	16.206.50	0.006061	1.90378	10.37820
16.0	16.206.96	0.004051	1.90377	15.23470
17.0	16.206.91	0.002041	1.90377	26.25600

TABLE 3.3

c_n for different α s. X $^1\Sigma_g^+$: Br₂

α	RMSD	$10^{-5}c_6$	$10^{-5}c_8$
-1.4	0.522	2.932	257.67
-1.2	0.373	5.554	204.47
-1.0	0.213	3.637	171.03
-0.8	0.078	3.877	147.64
-0.6	0.210	4.074	130.19
-0.4	0.436	4.238	116.57
-0.2	0.696	4.378	105.59

TABLE 3.4

c_n for different α s E $^3\Pi^-$: Br₂

α	RMSD	$10^{-5}c_6$	$10^{-5}c_8$
-0.4	0.129	8.24	104.2
-0.2	0.115	3.32	98.5
-0.0	0.112	3.39	93.4
+0.2	0.122	8.45	86.8
+0.4	0.144	3.51	84.7
+0.6	0.175	8.57	80.9
+0.8	0.212	8.62	77.4

Note : RMSD is in cm^{-1} . Units of c_6 and c_8 are given in the text.

CHAPTER 4

LONG-RANGE ANALYSIS OF Cl₂ AND I₂

The results of the long-range analysis of the X and B states of Cl₂ and X state of I₂ employing the same methods as those applied in the third chapter are given in this chapter. Then, conclusions drawn from the analyses of halogens, are presented.

B $^3\Pi$ (v_u^+) State of Cl₂

The absorption bands of the system B $^3\Pi$ - X $^1\Sigma_g^+$ were studied by several workers^{33,34,37} which provided very accurate information about energy levels $v' \geq 5$. Until recently, for the lower levels, low resolution band head measurements¹¹ were used for vibrational energies and rotational constants were obtained by extrapolation. Recently, Coxon and Shankar,³⁶ reported the rotational analysis of bands for the vibrational levels from 0 to 5. Using their data and earlier works,^{33,34,36} more accurate vibrational and rotational constants were obtained, in the present work. Also, the long-range analysis of the RKR potential computed from the data so obtained.

The vibrational term values T_v , (J=0) of the B state relative to X $^1\Sigma_g^+$ ($v=0$, J=0) were calculated from the relation

$$T_v, (J=0) = \nu_{v',v} + G_0(v) \quad (4.1)$$

where $\nu_{v',v}$ is the frequency corresponding to the vibrational transition $v' - v$ and $G_0(v)$ is the ground state vibrational term value, calculated from the Dunham coefficients³⁵ of the X state of Cl_2 . These were fitted to a polynomial of fourth order in v' by least squares for $0 \leq v' \leq 12$ and the zero point energy, 126.42cm^{-1} was calculated from the constants so obtained. The vibrational constants were then determined from the least squares fit of $G(v')$, for $0 \leq v \leq 12$ to the polynomial

$$G(v') = \sum_n C_n (v' + \frac{1}{2})^n ; \quad n = 1 \text{ to } 4 \quad (4.2)$$

The rotational constants B_v were taken from the work of Coxon and Shankar³⁶ for $v' \leq 4$ and from that of Clyne and Coxon³³ for $5 \leq v' \leq 29$. The gaps in the experimental B_v values were filled by values calculated from the fits of the available values to the equation

$$B_v = \sum_k B_k (v' + \frac{1}{2})^k ; \quad k = 0 \text{ to } 5 \quad (4.3)$$

The constants C_n and B_k are given in table 4.1 together with the dissociation energy $D = 3341.04\text{cm}^{-1}$.

Least squares fits of $G(v')$ in the range $25 \leq v' \leq 31$ (fig. 4.2) and B_v in the range $26 \leq v' \leq 29$, to the equations

$$[D - G(v')]^{3/10} = H_5 (v_D - v') \quad (4.4)$$

$$\text{and } [B_v]^{3/4} = Q (v_D - v') \quad (4.5)$$

and respectively were used to extrapolate the values of $G(v')$ and B upto the dissociation limit. As expected ⁴ $C_5 = 1.226 \times 10^5 \text{ cm}^{-1} \text{ A}^5$ calculated from H_5 is smaller than $(2.97 \times 10^5 \text{ cm}^{-1} \text{ A}^5)$, calculated from Q .

The RKR turning points were obtained using the observed vibrational energies in conjunction with the extrapolated ones given in table 3.2 and the B_v values calculated from eq. 4.3 for $v > 26$ and those calculated from eq. 4.5 for $27 \leq v \leq 35$. As explained in the previous chapter, the irregularities above $v \geq 23$, in the repulsive branch of the potential curve were removed and the attractive branch was adjusted appropriately. The turning points are given in table 4.2.

$\chi^1\Sigma_g^+$ State of Chlorine

A long series of doublets were observed by Rao and Venkateswarlu³² which were assigned to vibrational levels of the ground state over the range 0 to 54. From a long-range analysis of the vibrational spacings of this state, their last observed doublet was reassigned⁵ to $v = 55$ and the asymptotic value of n was obtained as 6.

Douglas and Hoy³⁵ studied the resonance series under higher resolution and computed the potential curve of the χ state. They showed that there was very good agreement between the

observed long-range portion of the potential and that calculated from the B state constants. However, when calculation was repeated using the revised B state constants obtained in the present work, it was found that there was no such agreement. Hence it was felt necessary to update the long-range analysis.

As the data of Douglas and Hoy are more precise and extensive than the data used by Le Roy,⁹ the long-range analysis of their vibrational spacings near the dissociation limit was repeated. With the dissociation energy 20276.44cm^{-1} , the vibrational levels from 56 to 58 were analysed. Surprisingly, the asymptotic value of n turned out to be 4 contrary to both the theoretical expectations and the experimental value obtained from the earlier data.

Further, the plot of $[D - G(v)]^{(n-2)/2n}$ vs. v (fig. 4.3) shows a pronounced positive curvature for the highest observed vibrational levels with $n = 6$, while a similar plot with $n = 4$ is linear. Also, of the two plots (fig. 4.4) of $G(v)$ vs. $(\Delta G)^{2n/(n+2)}$ with $n = 6$ and 4, only the latter is linear yielding an estimate of D almost equal to the known value. Thus the graphical evidence is also in favour of $n = 4$. As a value of $n = 6$ has been obtained from the long-range analyses of the X states of Br_2 and I_2 , there is no reason to believe that it will be

different for the X state of chlorine.* So, in order to extrapolate the vibrational energies and the B_v values of this state from $v = 59$ upto the dissociation limit least squares fits to eqs. 1.23 and 1.24 with $n = 6$ were used. With these extrapolated $G(v)$ and B_v values in conjunction with those observed (given in table 4.4) the RKR potential was computed. The RKR turning points after correcting for irregularities in the repulsive branch above $v = 45$, are given in table 4.3.

$X \sum_g^4$ State of Iodine

Koffend et al.⁴¹ studied the X state of iodine near dissociation using optically pumped continuous wave iodine laser. They observed transitions involving the levels from $v = 83$ to 96 and carried out the long-range analysis of the five highest observed levels. C_6 was evaluated using a theoretical value of $n = 6$ for the asymptotic power. Tellinghuisen et al.,⁴² from their work on D-X fluorescence spectrum of I_2 extended the experimental data upto $v = 99$. Their vibrational spacings in the range $93 \leq v \leq 99$ were fitted by least squares to eq. 1.22 for

* This deviation perhaps arises out of vibrational misassignment or wrong identification of resonance doublets in the region near dissociation.

different values of n and the results are given in table 4.5. A cursory examination of standard deviations and resultant dissociation energies of different fits shows that the value of $n = 6$, in agreement with the theoretical value. The $G(v)$ and B_v values were then extrapolated from $v = 99$ to dissociation limit (corresponding to the integer vibrational index 114, fig. 4.5) with $n = 6$. The RKR turning points appropriately corrected for irregularities in the inner branch above $v = 88$ were computed in the same way in which those corresponding to the X states of chlorine and bromine were computed. These are given in table 4.6.

Before proceeding with the long-range analyses of these states it was ascertained that their Birge-Spooner plots (fig. 4.1) show positive curvature for levels lying close to dissociation limit, which is a necessary condition for the applicability of the methods employed in the long-range analysis.

Long-range Analysis

The analyses of RKR turning points of X states of Cl_2 and I_2 and B state of Cl_2 were performed for the levels lying outside the electron overlap region⁴

and the results are summarised in tables 4.8 and 4.10.*

The turning points in the ranges $23 \leq v \leq 31$ and $55 \leq v \leq 62$ for B and X states of Cl_2 respectively were fitted by least squares to eqs. 1.30, 1.31 and 1.32 with appropriate values of n. Similarly, those in the range $97 \leq v \leq 109$ for X state of I_2 were analysed. In these fits, values of α in the range -1.4 to -0.6 for X states and -0.6 to +0.6 for B states were used. The range of turning points, the critical distances $r_b(\text{X}_2)$, c_5 values, and dissociation energies for B state halogens are given in table 4.9. and similar data for X state halogens are given in table 4.7. The results of the least-square fits of X state halogens along with σ 's (root mean square deviations) for different values of α are given in table 4.8 and those of the B state halogens are presented in table 4.10. To complete the picture of the B state halogens the long-range analysis of the B state of iodine, reported by Danyluk and King³⁸ was included in these tables.

* The long-range analysis of the state of I_2 presented here is warranted inspite of that by Bacis et al.⁴⁴ with higher resolution data, for the reasons. 1) The lower limit of the long-range analysis was inside the overlap region, where eq. 1.15 is not valid. 2) No reasons were offered for neglecting coefficients higher than c_3 in their analysis. Hence, the long-range analysis performed with the best available data,⁴² is given here.

The optimum value of α should normally be that value of α for which the σ of the fit is minimum. For the X states of halogens, the optimum value ought to be -1.6, -0.8 and -1.2 for Cl_2 , Br_2 and I_2 respectively. It may be noted here that the value of -1.6 for Cl_2 is uncertain in view of the monotonical variation of σ with α . However, there is a further constraint in choosing the optimum value of α ; for any given state of halogens, the value of α should be the same. Applying this criterion it is therefore concluded that $\alpha = -1$ represents the effective contributions from higher terms to the long-range potentials of the X state halogens. Similar considerations unambiguously lead to the conclusions that $\alpha = 0$ best represents the long-range potentials of B state halogens. The values of the constants C_6 and C_8 considered to be the most probable values for these two states are also given in tables 4.8 and 4.10. For the sake of comparison theoretical estimates of C_6 values are included in the table 4.10. The agreement between the theoretical and the most probable values of C_6 of the B state is quite gratifying.

The RKR turning points were analysed also by directly fitting them to eq. 1.33 in the range in which the earlier analyses using Le Roy's generalised equations were made. Two sets of constants were obtained one from the fits to the three-term version of eq. 1.33 ($C_{10} \neq 0$)

and the other from the fits to the two-term version ($C_{10} \equiv 0$). The results of the fits with σ 's are given in tables 4.11 and 4.12 for the X and B states of halogens respectively.

The optimum value of $\alpha = -1$ for the X states of halogens indicates that C_{10} , which collectively denotes the contributions to the long-range potential from higher terms is zero. It is therefore expected that the first set of constants in table 4.11 should agree with the most probable value of the constants given in table 4.8. The agreement is indeed very close. However, for Br_2 , the σ of the fit to the three-term version of the equation is small enough to warrant the adoption of the constants obtained from this fit.

In the case of B states of halogens the optimum value of α turned out to be zero in agreement with Le Roy's recommended value for this state. This value of α indicates a non zero value for C_{10} . So one expects that the second set of constants obtained from the fits to the three-term version of the equation should agree with the most probable values given in table 4.10. Although this is readily seen to be the case for B states of bromine and iodine, it is not so for that of chlorine. C_{10} has a negative value which is totally unexpected, as the second order terms for species formed of ground state atoms are

necessarily attractive. Further, the first set of constants agree better with the most probable values than the second set of constants, besides giving a lower σ for the fit.

On comparing the constants obtained by extending the range of r_2 values upto about 15A, with the corresponding constants given in tables 4.8 and 4.10, it is found that the constants are range-dependent. Thus it is not possible to determine a unique set of constants by either of these methods. However any one of the methods may be used, with more or less, equal validity.

The ratio of the first two terms in the expansion of the potential for both X and B states were calculated in the range $5 \leq r \leq 20$ A and given in table 4.13. Examination of the table shows that the contribution from C_6/r^6 is really high compared to C_8/r^8 for the X states and hence the extrapolation of the energy levels by eq. 4.4 with $n = 6$ is well justified. Though, the results are not so encouraging in the case of the B states eq. 4.4 still gives a good approximation for, the potential $C_5/r^5 + C_6/r^6$ would lead to the same equation, only C_5 is not pure.⁹

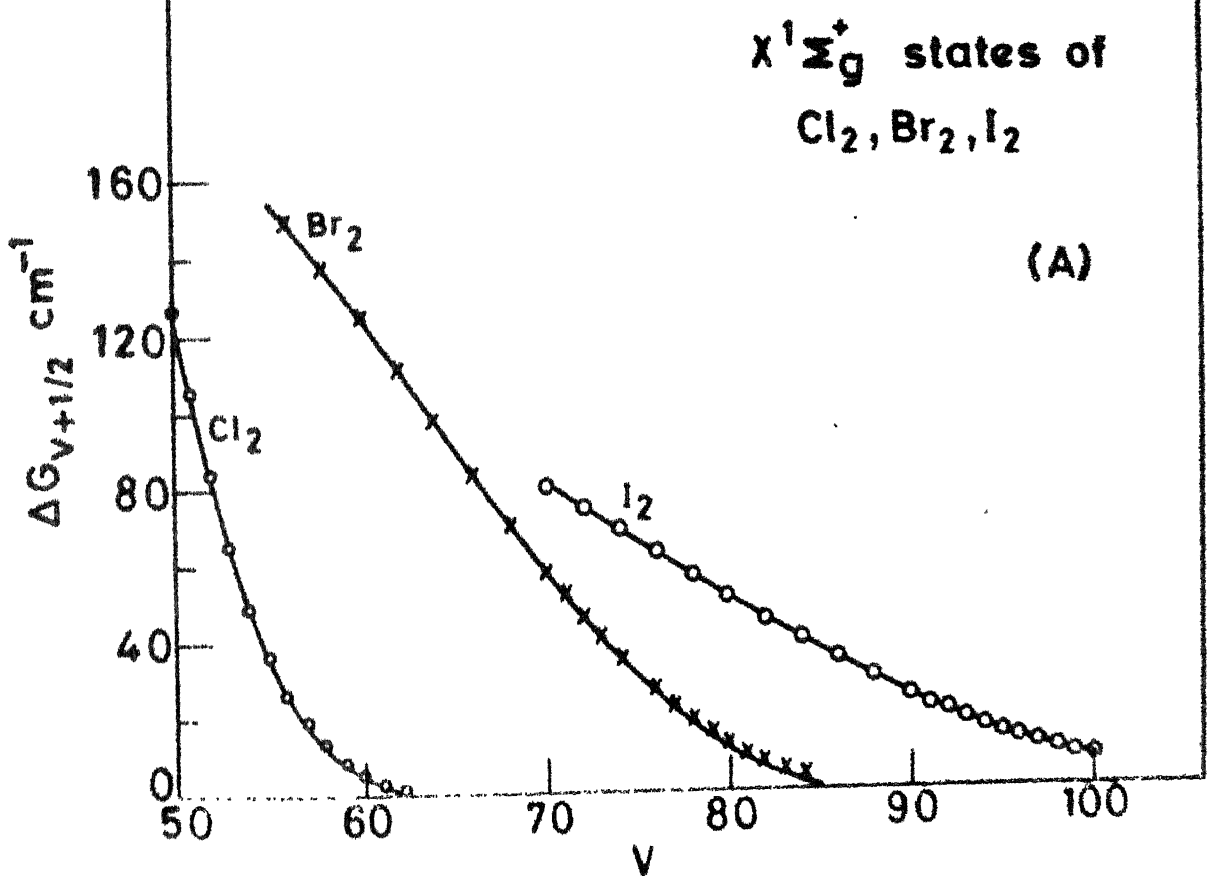
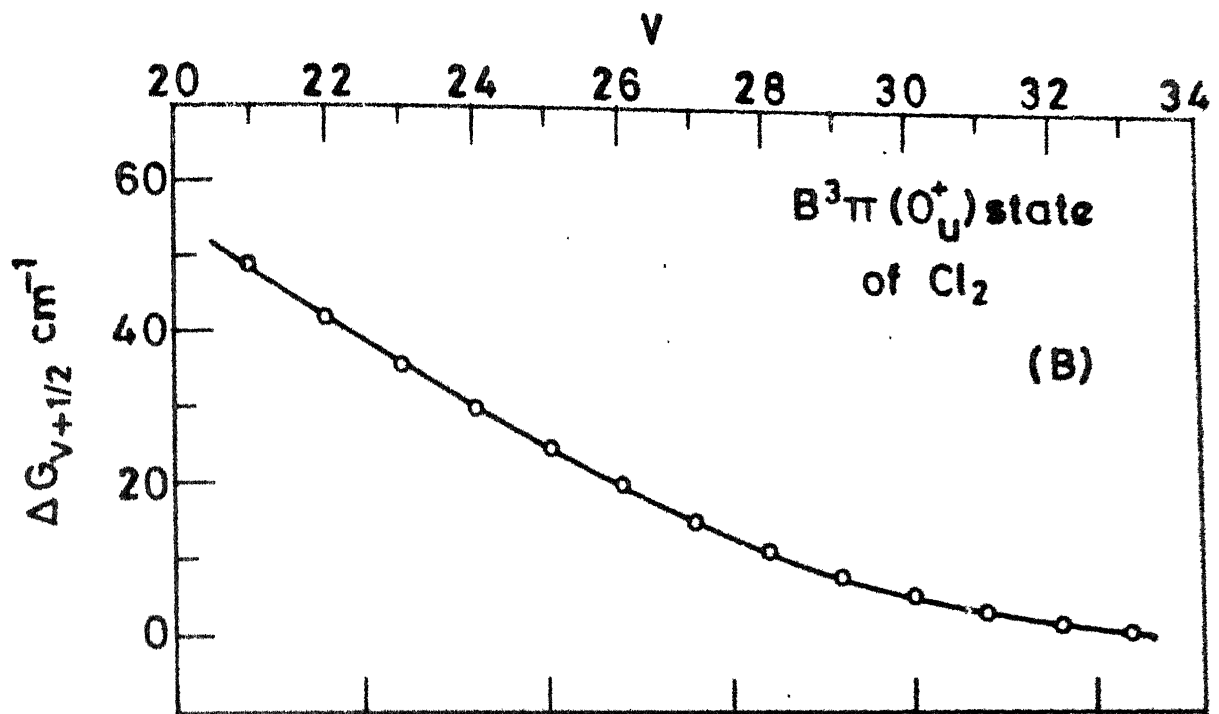


Fig. 4.1 Birge-Spooner plots for the X states of Cl_2, Br_2

$\text{Cl}_2 \text{ B } ^3\pi(\text{O}^+_u)$

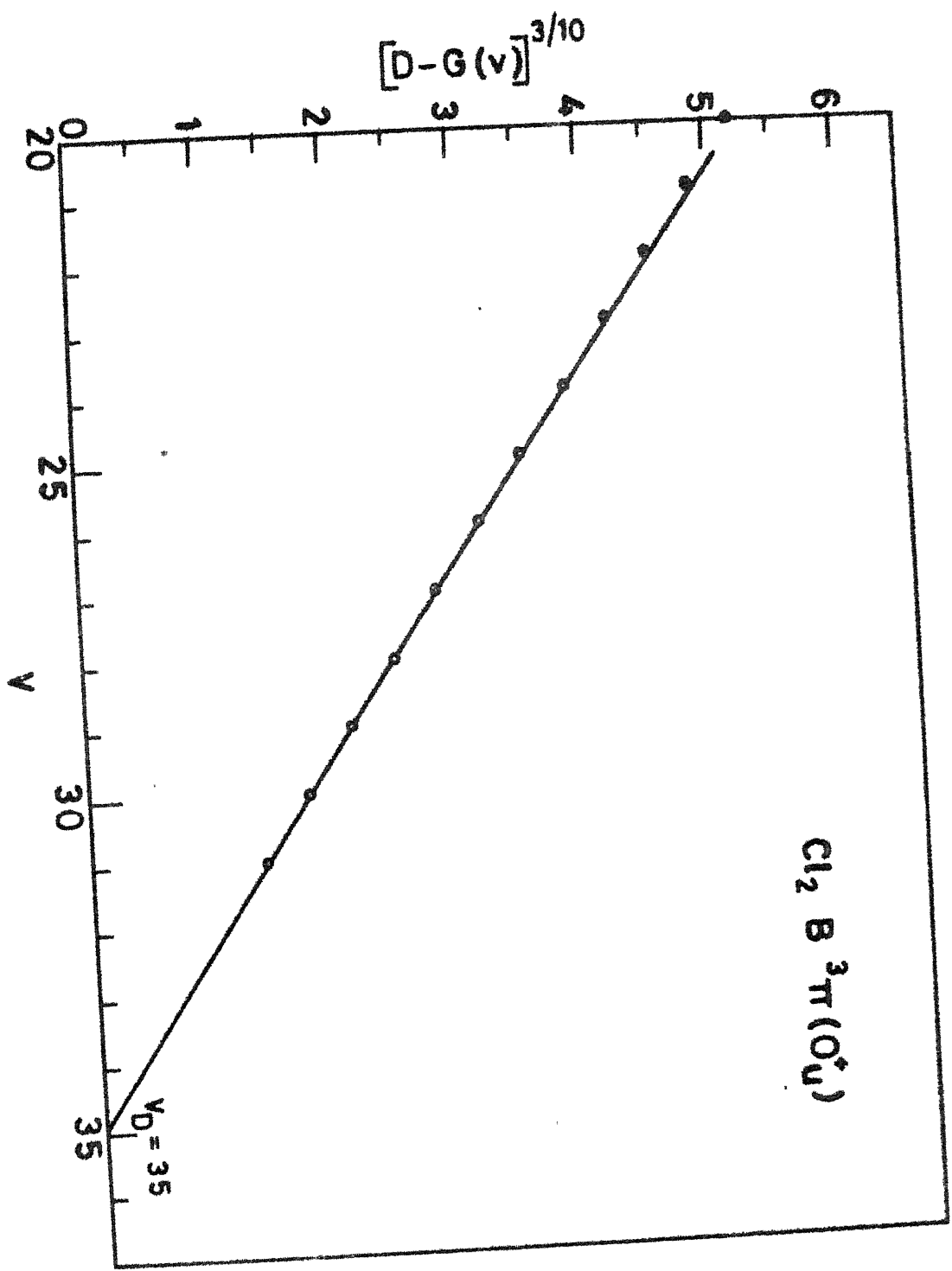


Fig. 4.2 Plot of $[D - G(v)]^{3/10}$ vs. v for the B state of Cl_2 . The units of $[D - G(v)]$ are cm^{-1} . The plot is linear with an intercept

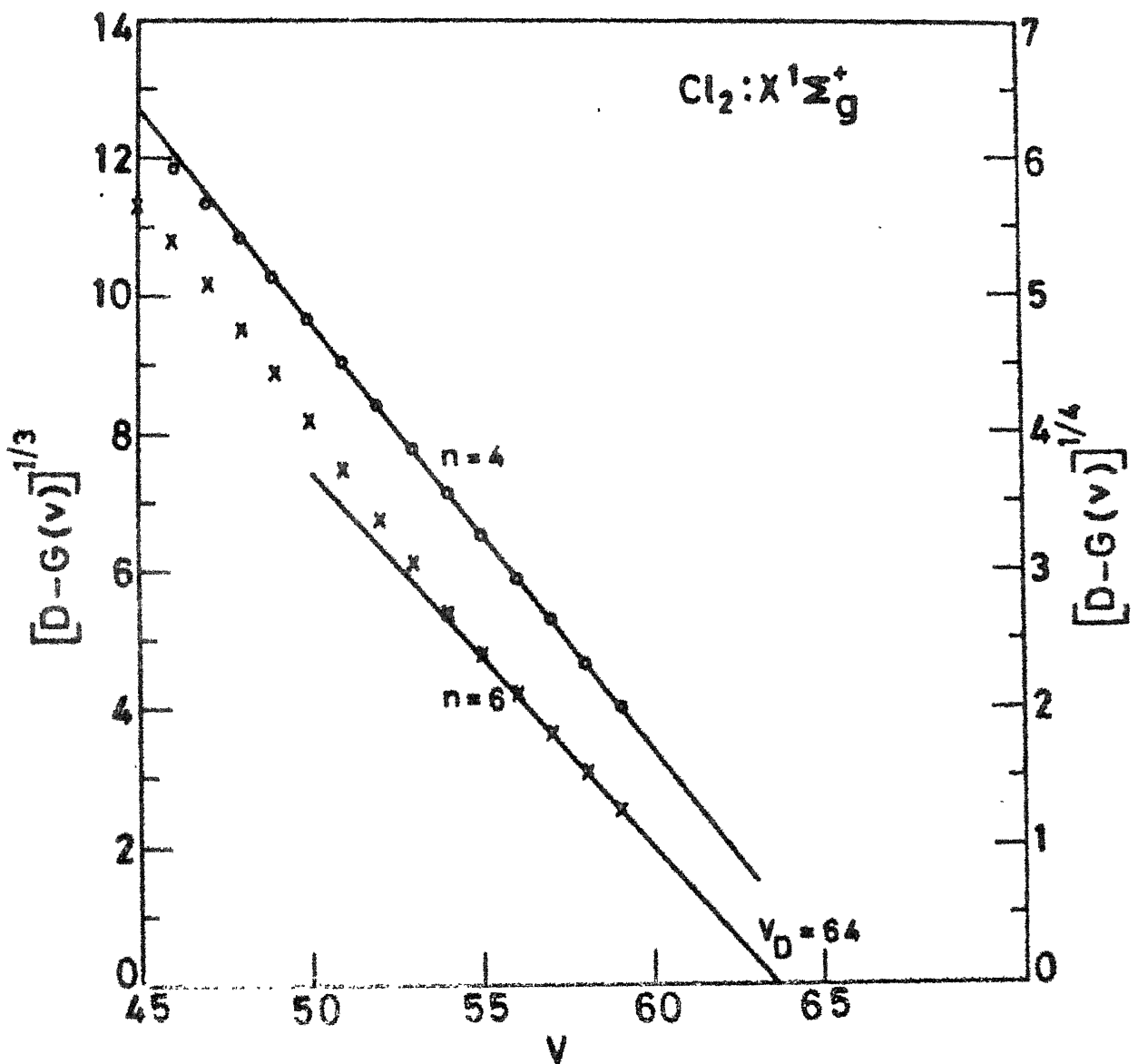


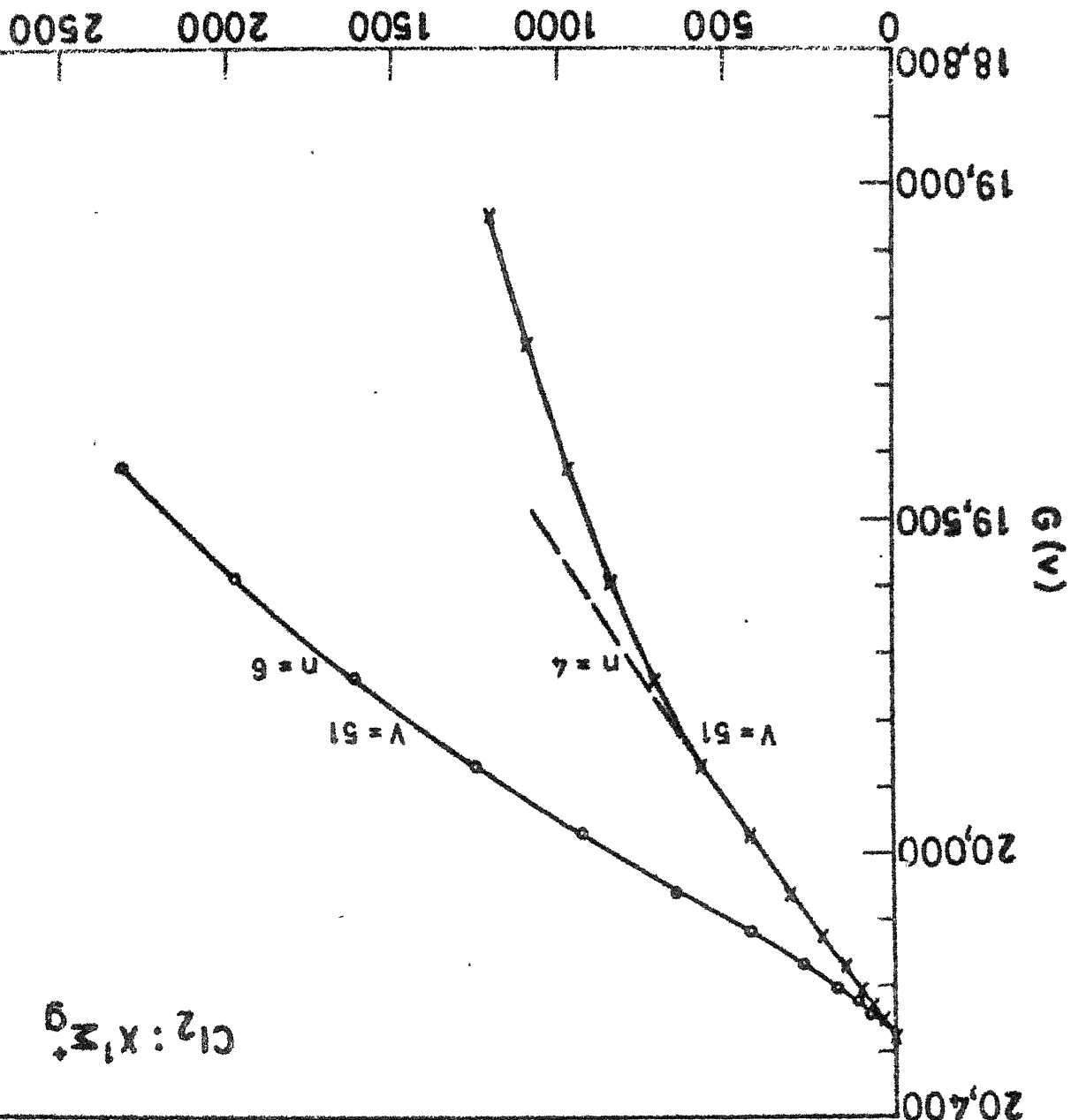
Fig. 4.3 The plots of $[D - G(v)]^{(n-2)/2n}$ for $n = 4$ and 6 of the X state of Cl_2 . The plot with $n = 4$ is linear while that with $n = 6$ shows a positive curvature.

$n = 4$ is linear above $V = 51$.

With $n = 6$ and 4 as indicated. The plot corresponds to

Fig. 4.4 Plots of $G(V) - (\Delta G)_{2n/(n+2)}$ for the X state of C_2

$$(\Delta G)_{2n/(n+2)}$$



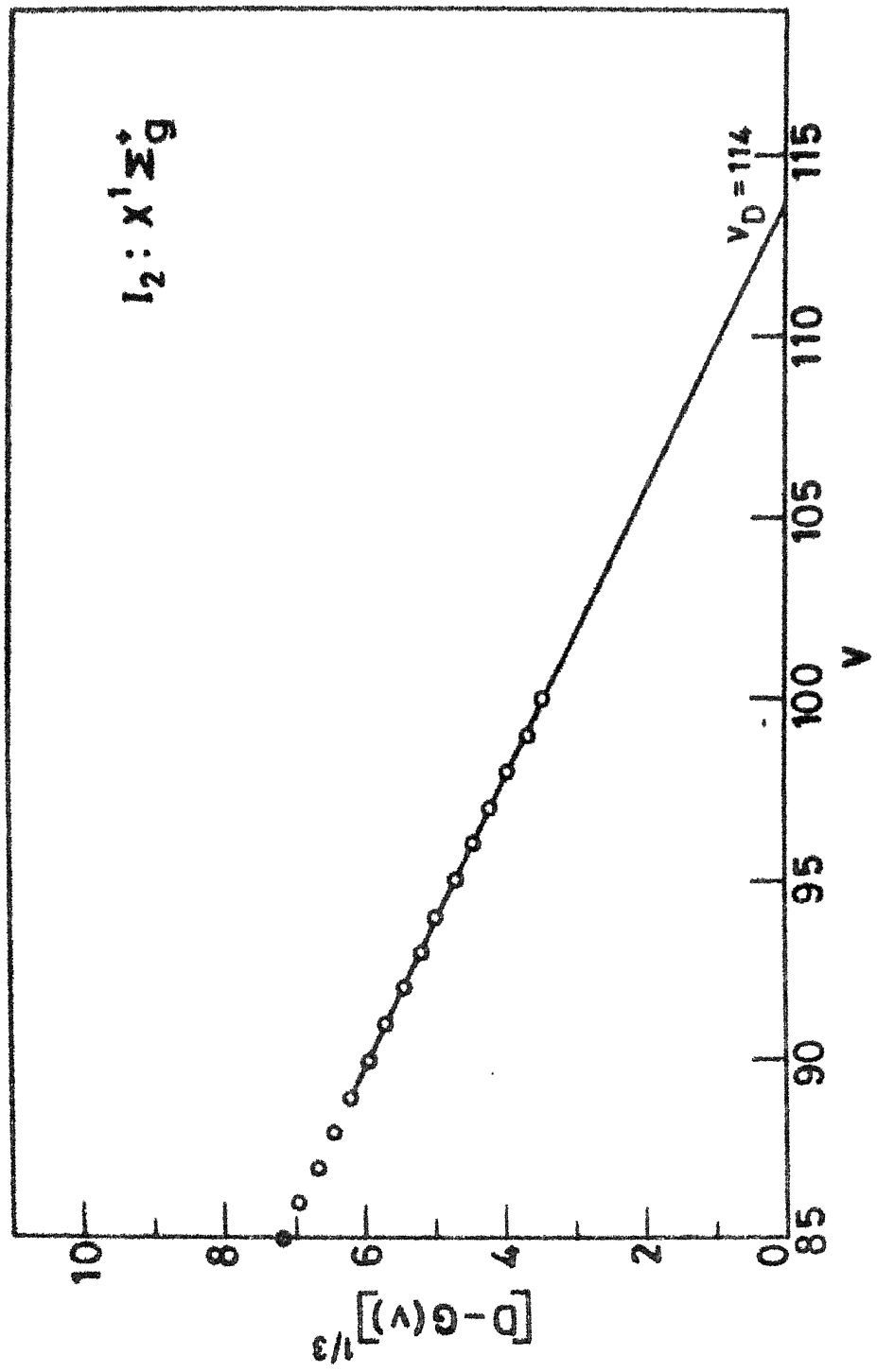


Fig. 4.5 Plot of $[D - G(v)]^{1/3}$ vs. v for the X state of I_2 .
The molecule dissociates at $v_D = 114$.

TABLE 4.1

Molecular Constants of Chlorine (B State)

w_0	=	250.583	$w_0 x_0$	=	4.533
$w_0 y_0$	=	-0.06227	$w_0 z_0$	=	-0.0015208
$G(0)$	=	126.42			
D^+	=	3341.04			

$\omega = v \approx 12$

c_1	=	255.095	c_2	=	4.4379
c_3	=	-0.06573	c_4	=	-0.0015503

$\omega = v \approx 12$

b_0	=	1.0515×10^{-1}	b_1	=	-2.4556×10^{-3}
b_2	=	-2.0312×10^{-5}	b_3	=	-6.9709×10^{-6}
b_4	=	3.1169×10^{-7}	b_5	=	-4.5232×10^{-9}

 $\omega = v \approx 26$

[†] Calculated from the dissociation energy, 20879.64 cm⁻¹ (ref. 9). All constants are in cm⁻¹.

TABLE 4.2
RKR TURNING POINTS OF CHLORINE (B-STATE).

V	G(V)	BV	R1	R2
0	126.31	0.161900	2.35136	2.52634
1	372.32	0.159380	2.30082	2.60880
2	608.91	0.156770	2.26936	2.67370
3	835.76	0.154040	2.24569	2.73268
4	1052.59	0.151160	2.22660	2.78932
5	1259.14	0.148120	2.21065	2.84539
6	1455.21	0.144910	2.19704	2.90198
7	1640.64	0.141520	2.18529	2.95993
8	1815.28	0.137950	2.17504	3.01993
9	1979.03	0.134200	2.16591	3.08264
10	2131.85	0.130270	2.15800	3.14862
11	2273.71	0.126160	2.15098	3.21862
12	2404.62	0.123280	2.14249	3.29111
13	2524.91	0.117480	2.13602	3.36965
14	2634.73	0.112910	2.13354	3.45817
15	2734.50	0.108200	2.12829	3.54937
16	2824.62	0.103370	2.12535	3.65027
17	2905.51	0.098420	2.12147	3.75832

V	G(V)	Bv	R1	R2
18	2977.64	0.093360	2.11904	3.87725
19	3041.45	0.088180	2.11637	4.00745
20	3097.45	0.082910	2.11428	4.15106
21	3146.10	0.077530	2.11238	4.31131
22	3187.89	0.072040	2.11085	4.49104
23	3223.31	0.066420	2.10960	4.69521
24	3252.85	0.060680	2.10841	4.92974
25	3276.95	0.054790	2.10752	5.20591
26	3296.20	0.048720	2.10681	5.52979
27	3310.98	0.042600	2.10627	5.93902
28	3321.95	0.036470	2.10587	6.43403
29	3329.74	0.030580	2.10559	7.08088
30	3334.95	0.024970	2.10540	7.94378
31	3338.17	0.019650	2.10528	9.15637
32	3339.92	0.014680	2.10522	11.08021
33	3340.69	0.010100	2.10519	14.55945
34	3340.90	0.005990	2.10518	25.60096
35	3340.92	0.002510	2.10518	46.19419

TABLE 4.3
RK R TURNING POINTS OF CHLORINE (X-STATE).

V	G(V)	R1	R2
0	279.22	1.93134	2.04897
2	1382.50	1.86946	2.13464
3	1925.97	1.85056	2.16563
4	2463.95	1.83482	2.19360
5	2996.40	1.82122	2.21956
6	3523.29	1.80918	2.24411
7	4044.56	1.79833	2.26761
8	4560.16	1.78845	2.29029
9	5070.05	1.77936	2.31234
10	5574.17	1.77093	2.33390
11	6072.45	1.76308	2.35506
12	6564.85	1.75573	2.37591
13	7051.28	1.74880	2.39652
14	7531.70	1.74227	2.41694
15	8006.02	1.73607	2.43725
16	8474.18	1.73020	2.45745
17	8936.10	1.72460	2.47762
18	9391.69	1.71925	2.49778

V	G(V)	R1	R2
19	9840.87	1.71416	2.51798
20	10283.56	1.70928	2.53823
21	10719.66	1.70462	2.55860
22	11149.08	1.70015	2.57909
23	11571.70	1.69586	2.59976
24	11987.43	1.69175	2.62062
25	12396.14	1.68781	2.64173
26	12797.72	1.68402	2.66310
27	13192.03	1.68038	2.68479
28	13578.93	1.67689	2.70683
29	13958.29	1.67355	2.72926
30	14329.93	1.67034	2.75214
31	14693.69	1.66726	2.77551
32	15049.41	1.66431	2.79941
33	15396.87	1.66147	2.82394
34	15735.89	1.65875	2.84912
35	16066.23	1.65614	2.87507
36	16387.68	1.65365	2.90182
37	16699.97	1.65124	2.92951
38	17002.85	1.64893	2.95821
39	17296.03	1.64670	2.98808
40	17579.20	1.64455	3.01923
41	17851.87	1.64249	3.05204

V	S(V)	R1	R2
42	18113.56	1.64058	3.08673
43	18363.97	1.63873	3.12331
44	18602.77	1.63701	3.16222
45	18828.70	1.63529	3.20489
46	19041.27	1.63398	3.25089
47	19239.88	1.63262	3.30142
48	19422.57	1.63138	3.35970
49	19588.66	1.63027	3.42441
50	19736.00	1.62928	3.50339
51	19863.06	1.62845	3.59779
52	19968.55	1.62775	3.71700
53	20052.58	1.62720	3.86680
54	20117.72	1.62678	4.04820
55	20166.10	1.62647	4.28637
56	20202.21	1.62623	4.54673
57	20227.91	1.62607	4.91738
58	20246.90	1.62594	5.27071
59	20260.15	1.62586	5.83024
60	20268.70	1.62580	6.51762
61	20273.57	1.62577	7.61742
62	20275.81	1.62576	9.61271
63	20276.43	1.62575	16.37501

TABLE 4.4

$G(v)$, B_v of Cl_2 (X State), $G(v)$ and B_v are in cm^{-1}

v	$G(v)$	B_v
59	20260.13	0.041381
60	20268.68	0.032532
61	20273.55	0.023683
62	20275.79	0.014334
63	20276.41	0.005934

TABLE 4.5

n	$SD \text{ cm}^{-1}$	Dissociation energy cm^{-1}
4.5	2.48	12550.08
5.0	2.19	12549.06
5.5	2.07	12543.17
6.0	2.07	12547.38
6.5	2.16	12546.69
7.0	2.29	12546.07
7.5	2.43	12545.51

TABLE 4.6
RKR TURNING POINTS OF IODINE (X-STATE).

V	G(V)	Bv	R1	R2
0	107.10	0.037311	2.61846	2.71811
1	320.41	0.037196	2.58545	2.75847
2	532.48	0.037081	2.56370	2.78761
3	743.31	0.036965	2.54659	2.81217
4	952.91	0.036849	2.53219	2.83408
5	1161.25	0.036732	2.51963	2.85421
6	1368.33	0.036614	2.50841	2.87305
7	1574.15	0.036496	2.49823	2.89092
8	1778.68	0.036376	2.48889	2.90802
9	1981.93	0.036256	2.48024	2.92450
10	2183.88	0.036134	2.47217	2.94047
11	2384.53	0.036012	2.46451	2.95601
12	2583.86	0.035889	2.45749	2.97119
13	2781.86	0.035764	2.45075	2.98607
14	2978.52	0.035639	2.44435	3.00069
15	3173.84	0.035512	2.43826	3.01509
16	3367.79	0.035385	2.43245	3.02929
17	3560.38	0.035256	2.42689	3.04333

V	G(V)	Bv	R1	R2
18	3751.58	0.035126	2.42157	3.05724
19	3941.38	0.034995	2.41645	3.07102
20	4129.76	0.034863	2.41153	3.08470
21	4316.73	0.034730	2.40679	3.09830
22	4502.25	0.034595	2.40222	3.11184
23	4686.31	0.034459	2.39781	3.12532
24	4868.91	0.034322	2.39354	3.13876
25	5050.01	0.034183	2.38941	3.15217
26	5229.62	0.034043	2.38541	3.16557
27	5407.70	0.033902	2.38154	3.17896
28	5584.24	0.033759	2.37778	3.19236
29	5759.23	0.033614	2.37412	3.20578
30	5932.65	0.033468	2.37058	3.21922
31	6104.46	0.033320	2.36713	3.23270
32	6274.67	0.033170	2.36378	3.24623
33	6443.24	0.033018	2.36051	3.25982
34	6610.15	0.032864	2.35734	3.27348
35	6775.37	0.032708	2.35425	3.28721
36	6938.90	0.032550	2.35123	3.30104
37	7100.69	0.032389	2.34830	3.31496
38	7260.73	0.032225	2.34544	3.32900
39	7418.99	0.032059	2.34265	3.34316
40	7575.43	0.031890	2.33994	3.35746

V	G(V)	Bv	R1	R2
41	7730.04	0.031718	2.33729	3.37191
42	7882.77	0.031542	2.33471	3.38652
43	8033.61	0.031364	2.33220	3.40130
44	8182.52	0.031181	2.32975	3.41627
45	8329.46	0.030995	2.32736	3.43145
46	8474.40	0.030805	2.32504	3.44685
47	8617.31	0.030611	2.32277	3.46249
48	8758.16	0.030413	2.32057	3.47836
49	8896.89	0.030210	2.31842	3.49452
50	9033.49	0.030003	2.31634	3.51096
51	9167.90	0.029791	2.31431	3.52772
52	9300.40	0.029573	2.31233	3.54480
53	9430.03	0.029351	2.31041	3.56225
54	9557.66	0.029123	2.30855	3.58007
55	9682.94	0.028889	2.30674	3.59829
56	9805.84	0.028649	2.30499	3.61695
57	9926.31	0.028403	2.30328	3.63607
58	10044.30	0.028151	2.30163	3.65568
59	10159.78	0.027892	2.30003	3.67581
60	10272.69	0.027627	2.29848	3.69652
61	10383.00	0.027354	2.29697	3.71782
62	10490.65	0.027075	2.29551	3.73976
63	10595.62	0.026788	2.29410	3.76238

V	G(V)	Bv	R1	R2
64	10697.84	0.026493	2.29273	3.78574
65	10797.30	0.026191	2.29149	3.80988
66	10893.94	0.025881	2.29011	3.83485
67	10987.73	0.025563	2.28887	3.86070
68	11078.65	0.025236	2.28767	3.88751
69	11166.66	0.024901	2.28650	3.91533
70	11251.74	0.024557	2.28538	3.94424
71	11333.86	0.024204	2.28429	3.97429
72	11413.02	0.023843	2.28325	4.00559
73	11489.49	0.023472	2.28224	4.03820
74	11562.39	0.023092	2.28128	4.07221
75	11632.59	0.022702	2.28035	4.10775
76	11699.81	0.022303	2.27949	4.14489
77	11764.07	0.021894	2.27866	4.18377
78	11825.36	0.021475	2.27788	4.22452
79	11883.71	0.021046	2.27715	4.26728
80	11939.15	0.020607	2.27647	4.31222
81	11991.69	0.020157	2.27584	4.35951
82	12041.37	0.019598	2.27525	4.40939
83	12088.22	0.019228	2.27472	4.46206
84	12132.28	0.018747	2.27422	4.51785
85	12173.57	0.018255	2.27377	4.57704
86	12212.14	0.017753	2.27334	4.64004

V	G(V)	Bv	R1	R2
87	12248.03	0.017240	2.27293	4.70726
88	12281.29	0.016715	2.27252	4.77924
89	12311.95	0.016180	2.27217	4.85664
90	12340.11	0.015634	2.27184	4.94009
91	12365.81	0.015076	2.27155	5.03045
92	12389.13	0.014507	2.27128	5.12846
93	12410.29	0.013955	2.27104	5.23205
94	12428.93	0.013335	2.27083	5.35990
95	12445.79	0.012713	2.27064	5.47307
96	12460.97	0.012092	2.27047	5.61039
97	12474.55	0.011471	2.27031	5.75093
98	12486.63	0.010850	2.27018	5.90513
99	12497.29	0.010228	2.27006	6.07486
100	12506.62	0.009607	2.26995	6.26176
101	12514.70	0.008986	2.26986	6.47090
102	12521.64	0.008365	2.26978	6.70243
103	12527.51	0.007744	2.26972	6.96864
104	12532.41	0.007122	2.26966	7.26960
105	12536.41	0.006501	2.26961	7.52701
106	12539.63	0.005880	2.26958	8.03332
107	12542.13	0.005259	2.26955	8.54772
108	12544.01	0.004637	2.26953	9.16091
109	12545.35	0.004016	2.26951	9.98156

V	G(V)	Bv	R1	R2
110	12546.26	0.003395	2.26950	11.02194
111	12546.81	0.002774	2.26950	12.68091
112	12547.09	0.002152	2.26949	15.30744
113	12547.19	0.001531	2.26949	21.80208
114	12547.21	0.000910	2.26949	33.92981

TABLE 4.7

X	D cm ⁻¹	r _b (Å ₂)	r ₂ range	v range
Cl ₂	20276.44	4.11 Å	4.286-9.612 Å	55-62
Br ₂	15895.63	4.68 Å	4.759-3.646 Å	77-37
I ₂	12547.22	5.51 Å	5.751-9.932 Å	97-109

TABLE 4.8

ω	σ			$10^{-5} \sigma_5 \text{ cm}^{-1} \text{ Å}^6$			$10^{-5} \sigma_0 \text{ cm}^{-1} \text{ Å}^6$		
	Cl ₂	Br ₂	I ₂	Cl ₂	Br ₂	I ₂	Cl ₂	Br ₂	I ₂
-1.6	1.62	0.66	0.03	4.86	2.35	13.4	44.7	362	535
-1.4	1.65	0.52	0.05	4.37	2.93	13.5	42.7	258	477
-1.2	1.71	0.37	0.03	4.89	3.33	14.1	41.0	205	431
-1.0	1.76	0.21	0.04	4.90	3.64	14.4	30.4	171	393
-0.8	1.82	0.07	0.08	4.92	3.37	14.7	37.9	143	362
-0.6	1.87	0.21	0.11	4.93	4.07	14.9	36.4	130	335
-0.4	1.94	0.13	0.15	4.94	4.24	15.2	35.1	117	312
Most probable values				4.9	3.87	14.4	39.4	143	393

TABLE 4.9

χ	$\nu \text{ cm}^{-1}$	$10^{-5} \chi_{\text{C}_6}$ $\text{cm}^{-1} \text{\AA}^5$	$r_b (\text{\AA}_2)$ \AA	r_2 range \AA	v range
Cl_2	3341.04	1.226	4.1	4.695-9.156	25-31
Br_2	3839.61	1.818	4.7	4.963-8.363	39-52
I_2	20043.12	2.776	5.5	8.0 -15.3	77-82

TABLE 4.10

 C_6 and C_8 of B state Halogens

α	σ			$10^5 C_6 \text{ cm}^{-1} \text{\AA}^6$			$10^{-5} C_8 \text{ cm}^{-1} \text{\AA}^8$		
	Cl_2	Br_2	I_2	Cl_2	Br_2	I_2	Cl_2	Br_2	I_2
-0.6	0.16	0.15		4.39	3.16		48.6	111	
-0.4	0.14	0.13		4.43	3.24		45.0	104	
-0.2	0.12	0.12		4.46	3.32		43.3	98.4	
0.0	0.11	0.11		4.48	3.39	17.3 41.7	93.4 243		
0.2	0.11	0.12		4.51	3.45		39.8	38.3	
0.4	0.12	0.14		4.54	3.51		33.1	34.7	
0.6	0.13	0.17		4.56	3.57		30.5	80.9	
Most probable values				4.48	3.39	17.8 41.7	93.4 243		
Theoretical values				4.5	3.3	13.5			
				(0.5)	(0.3)	(2.0)			

TABLE 4.11

Constants from Direct fits, X State Halogens

Molecule	RMSD	c_6	c_8	c_{10}	α
Cl_2	1.309	3.70	134	-1490	-1.6
	3.79	4.51	53.1	0	
Br_2	1.293	3.17	223	-1130	-1.1
	0.173	3.59	173	0	
I_2	0.133	14.3	385	477	-0.9
	0.03	14.2	402	0	

TABLE 4.12

Constants from Direct fits, B State Halogens

Molecule	RMSD	c_6	c_8	c_{10}	α
Cl_2	0.43	4.32	57.3	-104	-1.2
	0.23	4.36	53.1	0	
Br_2	0.142	3.54	80.5	322	1.2
	0.53	3.11	121	0	

TABLE 4.13

The ratios of $(c_{n1}/r^{n1})/(c_{n2}/r^{n2})$

$r(\text{A})$	X states $(c_6/r^6)/(c_8/r^8)$			B States $(c_5/r^5)/(c_6/r^6)$		
	Cl_2	Br_2	I_2	Cl_2	Br_2	I_2
5	0.306	0.656	0.916	1.559	1.084	0.780
8	0.783	1.378	2.345	2.189	1.754	1.243
10	1.224	2.022	3.564	2.157	2.167	1.560
15	2.754	5.393	8.244	4.106	3.251	2.540
20	4.890	10.433	14.626	5.474	4.544	3.120

CHAPTER 5

ABSORPTION SPECTRUM OF BROMINE IN THE VACUUM ULTRAVIOLET

The vacuum ultraviolet spectrum of Br_2 was reported by Venkateswarlu⁴⁵ in which five Rydberg transitions converging to $85165 \pm 80 \text{ cm}^{-1}$ ($10.56 \pm 0.01 \text{ eV}$) were identified. This limit has been attributed to the ionisation energy of $^2\Pi_{3/2}$, of Br_2^+ . Further, two limits at 1180 and 1185 Å are reported as corresponding to the ionisation of the molecule from $v = 1$ and 2 of the ground state respectively. Based on the then existing value for $^2\Pi_{3/2} - ^2\Pi_{1/2}$ separation 3146 cm^{-1} , obtained by Frost, McDowell and Vroom,⁴⁹ he identified four more series converging to 23306 cm^{-1} leading to $^2\Pi_{1/2}$.

Recent photoionisation studies^{46,47} gave an ionisation potential $10.52 \pm 0.01 \text{ eV}$ leading to $^2\Pi_{3/2}$ of Br_2^+ . The difference between this value and that of Venkateswarlu corresponds to one vibrational quantum of the upper state and hence it was inferred that the ionisation limit obtained by him corresponds to the first vibrationally excited state of the ion. Cornford, Frost, McDowell, Ragle and Stenhouse,⁴⁸ from their studies on photoelectron spectra obtained the doublet separation

2320cm^{-1} as compared with the earlier value 3146cm^{-1} (Incidentally the difference corresponds to one vibrational quantum of the ground state). To resolve the existing discrepancies between the results of the vacuum ultraviolet spectrum and the photoelectron, photoionisation spectra, the spectra reported by Venkateswarlu are reinvestigated.

In the present analysis three possibilities were investigated to settle the above problems:

1. Keeping $\psi_5(0,0)$ of d, h, k, p, q series at the old values, the ionisation potential was changed to 34844cm^{-1} and the spectra were searched for higher members.
2. Search was made for a set of totally different members for series d, h, k, p, q.
3. The old O-l was assigned C-O in the present work and correspondingly Rydberg transitions were reassigned.

The ionisation potential 34844cm^{-1} reported by Dibeler et al⁴⁶ is 323cm^{-1} smaller than that reported by Venkateswarlu. The O-O bands of d_5 , h_5 , k_5 , p_5 and q_5 have been kept at their old values 66227cm^{-1} , 68651cm^{-1} , 70913cm^{-1} , 73459cm^{-1} , 74161cm^{-1} and the higher members of the series are evaluated using the ionisation potential

84844cm^{-1} . The result of the investigation for higher members is that either they are not found or they are very weak. Even the ones corresponding to $n = 6$ were difficult to identify. Hence the conclusion that the series starting with the above 0-0 for $n = 5$ converging to 84844cm^{-1} do not exist.

A second alternative is pursued in the present work to see if the analysis could be improved, following a heuristic procedure to identify the series d, h, k, p and q. Several intense bands have been picked up as the starting members of the series and the higher members calculated from the ionisation potential 84851cm^{-1} . The spectra are then searched for the series so calculated and the series with the following starting members have been identified: 66227cm^{-1} for d; 63651cm^{-1} for h; 70913cm^{-1} for k; 73459cm^{-1} for p and 74161cm^{-1} for q. The members of the series in this case are either moderately strong or weak; the intensities of the bands fluctuate and do not follow an order. These are represented by

$$\nu = 84851\text{cm}^{-1} - R/(n - \delta)^2, \quad n = 5, 6, \dots$$

with $\delta = 2.578, 2.404, 2.202, 1.896, 1.796$ for the series d, h, k, p and q respectively.

The temperature dependence of the intensities of the thresholds studied by Libeler et al.,^{46,47} concludes

that the limit 1174A (85165cm^{-1} , the limit of I_{∞} , reported by Venkateswarlu) corresponds to that of the first vibrationally excited state of the ion. Hence, all O-O bands assigned by Venkateswarlu were reassigned 1-0 in the present work. Thus, both the absorption and photoionisation spectra yield the same limit. The O-O bands are weaker than 1-0 bands, which happens especially when r_e , the equilibrium internuclear distances of the states involved in transitions are not equal. Accordingly some of the higher O-O bands are missing. The new assignments are given in tables 5.1 - 5.5. They are represented by

$$\nu = 34844\text{cm}^{-1} - R/(n - \delta)^2 ,$$

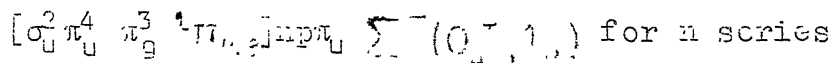
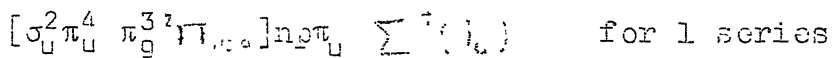
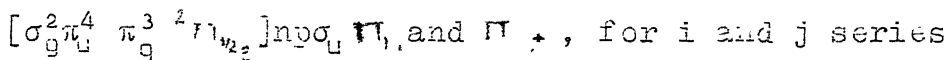
where $\delta = 2.593, 2.422, 2.225, 1.933$ and 1.842 respectively for the series d, h, k, p and q.

Of the second and the third analyses the third is preferred. In the second case, the reason for the fluctuation of intensities is not known. But in the third case, assuming that O-O bands are weak, everything follows automatically. This assumption that the overlap integral is smaller for O-O bands than for 1-0 bands, is quite reasonable, as the upper states may have larger r_e . Hence the analysis with old O-O bands reassigned to 1-0, is accepted in the present work.

In light of the value 2320cm^{-1} for the separation of the $^2\Pi_{\frac{3}{2}}$ components, series i, j, l and n converging to $^2\Pi_{\frac{1}{2},g}$ state of Br_2^+ ion have been reidentified. Only the members with $n = 5, 6$ and 7 have been located. The series are represented by

$$\nu = 87664\text{cm}^{-1} - R/(n - \delta)^2$$

where $\delta = 2.59, 2.55, 2.42, 2.40$ for i, j, l and n series respectively. As reported,⁴⁵ the electronic configurations and states of the series i, j, l and n are,



The observed and calculated $\Delta(\nu, 0)$ values agree well with each other. The doublet separation ($^2\Pi_{\frac{3}{2},g} - ^2\Pi_{\frac{1}{2},g}$) comes out to be 2320cm^{-1} , as expected.

The configuration $[\sigma_g^2 \pi_u^4 \pi_g^3 {}^2\Pi_{\frac{1}{2},g}] \sigma_u$ under $\Omega-\omega$ coupling gives the states Π_1 , Π_0 and Π_{-1} , of which the first two can have transitions from the ground state which are probably responsible for series i and j; of the states $-\sum^+(l_u, 0_u^-)$ and $\sum^-(l_u, 0_u^+)$,

transitions from ground state are possible to $\Sigma^+(l_u)$, $\Sigma^-(l_u, O_u^+)$ which are probably responsible for l and n series.

The assignments of $^2\Pi_u$ components by Venkateswarlu remain unaltered, for no members of the series other than the first were identified. Thus 71706cm^{-1} involves Π_{l_u} for its upper states and 74651cm^{-1} and 74768cm^{-1} involves Π_{l_u} and $\Pi_{O_u^+}$ for upper states respectively, which belong to $^2\Pi_u$ core.

All the stable electronic states of Br_2 are given in table 5.6. The states reassigned in this work are marked with asterix in the table.

TABLE 5.1

Rydberg Series d

TABLE 5.2

Rydberg Series h

n	Cal.	Obs.	w_0	n	Cal.	Obs.	w_0
5	65907	65907	320	5	68350	68350	321
6	75391	75360	352	6	76271	76280	319
7	79194	79190	323	7	79507	79574	292
8	31090	31067	321	8	31317	31281	
9	32170			9	32307	32298	329
10	32843	32885	(266)	10	32933		
11	83291			11	83352	33341	321
12	83604	83594	311	12	83643	33662	321
13	83830	83830	298	13	83863	83830	
14	84000	84014		14	84025	84025	
15	34131	34128		15	84150	84123	
16	84255	84226		16	84249		
17	84315			17	84327	84333	
18	84332	84382		18	84392	84382	
19	84436	84441		19	84445	84441	
20	84482	84472		20	84438	84472	

TABLE 5.3

Rydberg Series k

n	Cal	Obs	w _o
5	70596	70596	317
6	77144	77158	320
7	80032	80032	295
8	81554	81543	-
9	82453	82466	321
10	83029	83045	-
11	83419	83420	-
12	83696	83703	-
13	83899	83905	-
14	84053	-	-

TABLE 5.4

Rydberg Series p

n	Cal	Obs	w _o
5	73136	73138	321
6	73192	78181	315
7	80560	-	-
8	81857	-	-
9	82643	82659	329
10	85155	83151	-
11	83507	83434	-
12	83760	83751	-
13	83942	83941	-
14	84089	84097	-

TABLE 5.5

Rydberg Series q

n	Cal	Obs	w _o
5	73839	73839	322
6	78490	78490	362
7	80718	80747 (203)	
8	81949	81903	-
9	82702	82724	-
10	83195	83170	-

TABLE 5.6

Observed stable electronic states of Br_2

Configuration	Electronic states Case a or b type coupling	Case c or Ω ω coupling	Position of the System levels T_0 cm^{-1}	ω_0 cm^{-1}	$\omega_0 \times_0$ cm^{-1}
$[\sigma_g^2 \pi_u^4 \pi_g^3]^2 \Pi_{g,g}$	$5f\pi_u$	$\Sigma^-(0_u^+, 1_u)$	v	77639	303
$[\sigma_g^2 \pi_u^4 \pi_g^3]^2 \Pi_{g,g}$	$5f\pi_u$	$\Sigma^+(1_u)$	u	77491	374
$\sigma_g \pi_u^3 \pi_g^4 \sigma_u^2$	$^1\Pi_u$	1_u	N	76491	230
$[\sigma_g^2 \pi_u^4 \pi_g^3]^2 \Pi_{g,g}$	$5s\sigma_g$	$\Pi_{0u}+$	t	74768	299
$[\sigma_g^2 \pi_u^4 \pi_g^3]^2 \Pi_{g,g}$	$5s\sigma_g$	Π_{1u}	s	74651	303
$[\sigma_g^2 \pi_u^4 \pi_g^3]^2 \Pi_{g,g}$	$5f\sigma_u$	Π_{0u}	r	74455	341 (1.0)
$[\sigma_g^2 \pi_u^4 \pi_g^3]^2 \Pi_{g,g}$	$5f\delta_u$	$\Pi_{1,0}^+$	q *	73339	322
$\sigma_g \pi_u^3 \pi_g^4 \sigma_u^2$	$^3\Pi_u$	1_u^+	M	74013	241 (0.3)
$[\sigma_g^2 \pi_u^4 \pi_g^3]^2 \Pi_{g,g}$	$5f\pi_u$	$\Sigma^-(0_u^+)$	p *	73138	321
$[\sigma_g^2 \pi_u^4 \pi_g^3]^2 \Pi_{g,g}$	$5f\pi_u$	$\Delta(1_u)$	o (73240)		
$\sigma_g \pi_u^3 \pi_g^4 \sigma_u^2$	$^3\Pi_u$	1_u	L	72574	215
$[\sigma_g^2 \pi_u^4 \pi_g^3]^2 \Pi_{g,g}$	$5p\pi_u$	$\Sigma^-(0_u^+, 1_u)$	n *	71383	316
$[\sigma_g^2 \pi_u^4 \pi_g^3]^2 \Pi_{g,g}$	$5s\sigma_g$	Π_{1u}	m	71705	323
$[\sigma_g^2 \pi_u^4 \pi_g^3]^2 \Pi_{g,g}$	$5p\pi_u$	$\Sigma^+(1_u)$	l *	71158	
$[\sigma_g^2 \pi_u^4 \pi_g^3]^2 \Pi_{g,g}$	$5p\sigma_u$	Π_{1u}	k *	70596	317
$[\sigma_g^2 \pi_u^4 \pi_g^3]^2 \Pi_{g,g}$	$5p\sigma_u$	Π	j *	69396	338
$[\sigma_g^2 \pi_u^4 \pi_g^3]^2 \Pi_{g,g}$	$5p\sigma_u$	Π_{1u}	i *	68814	324
$[\sigma_g^2 \pi_u^4 \pi_g^3]^2 \Pi_{g,g}$	$5p\pi_u$	$\Sigma^+(0_u^+)$	h *	63330	321
$[\sigma_g^2 \pi_u^4 \pi_g^3]^2 \Pi_{g,g}$	$5p\pi_u$	$\Sigma^-(0_u^+)$	g	63603	339
$\sigma_g \pi_u^3 \pi_g^4 \sigma_u$	$(^1\Sigma_u^+)$	Σ_u^+	K		
$[\sigma_g^2 \pi_u^4 \pi_g^3]^2 \Pi_{g,g}$	$5d\sigma_g$	$\Pi_{2,1g}$	f	66500	430
$[\sigma_g^2 \pi_u^4 \pi_g^3]^2 \Pi_{g,g}$	$5p\pi_u$	$\Delta(1_u)$	e	66473	331
$[\sigma_g^2 \pi_u^4 \pi_g^3]^2 \Pi_{g,g}$	$5p\sigma_u$	Π_{1u}	c *	65907	320
			c	(62266)	(293)

TABLE 5.6 (Continued)

Configuration	Electronic states Case a or b type coupling	Case c or $\Omega-\omega$ coupling	System	Position of the levels cm ⁻¹	ω_a cm ⁻¹	$\omega_0 \times_0$ cm ⁻¹
$\sigma_g \pi_u^4 \pi_g^3 \sigma_u^2$	$^1\Pi_g$	1_g	J	61444	220	
			b	(60879)	(426)	
			I	(59855)	(281)	
$\sigma_g \pi_u^4 \pi_g^3 \sigma_u^2$	$^3\Pi_g$	1_g or 0_g^+	H	56669	106.5	1.5
$\sigma_g \pi_u^4 \pi_g^3 \sigma_u^2$	$^3\Sigma^-$	0_u^+	G	56303	255	
$[\sigma_g^2 \pi_u^4 \pi_g^3]^2 \Pi_{g,u}$] $5s \sigma_g$		$\Pi_{g,u}$	a	55534	330	
$\sigma_g \pi_u^4 \pi_g^3 \sigma_u^2$	$^3\Sigma^-$	1_u	F	52090	120	
$\sigma_g \pi_u^4 \pi_g^3 \sigma_u^2$	$^1\Sigma_g^+$	0_g^+	E	51715	149.2	1.15
$\sigma_g \pi_u^4 \pi_g^3 \sigma_u^2$	$^3\Sigma_g^-$	(1_g or 0_g^+)	D	43435	161.7	0.29
$\sigma_g \pi_u^4 \pi_g^3 \sigma_u$	$^3\Sigma^+$	1_u	v	(47000)		
$\sigma_g^2 \pi_u^4 \pi_g^3 \sigma_u$	$^3\Pi_u$	0_u^+	B	15340	160.1	1.84
			A	13815	150	2.7
$\sigma_g^2 \pi_u^4 \pi_g^4$	$^1\Sigma$		O	523.4	1.10	

NOTE : Rydberg states are designated by small letters, a, b, c. Valence or non-Rydberg states are designated by capital letters A, B, C. The values given in parentheses are either uncertain or approximate.

BIBLIOGRAPHY

1. H. Margenau and N.R. Kenster, 'Theory of Intermolecular Forces', 2nd Ed. (Pergamon Press, New York 1977).
2. J.O. Hirschfelder, C.F. Curtiss and R.B. Boyd, 'Molecular Theory of gases and liquids' (John Wiley, New York, 1954).
3. T.Y. Chang, Rev. Mod. Phys. 39, 911 (1967).
4. R.J. Le Roy, 'Molecular Spectroscopy', Vol. I, pp. 113-176, Eds. R.F. Barrow, D.A. Long, and D.J. Miller, The Chemical Society, Barlington House, London 1973).
5. R.J. Le Roy and R.B. Bernstein, J. Mol. Spectr. 37, 109 (1971).
6. R.J. Le Roy, J. Chem. Phys. 52, 2683 (1970).
7. R.J. Le Roy, Can. J. Phys. 50, 953 (1972).
8. J.A. Coxon, J. MoRT, 11, 443 (1971).
9. R.J. Le Roy, Can. J. Phys. 52, 246 (1974).
10. R.J. Le Roy and R.B. Bernstein, J. Chem. Phys. 52, 3369 (1970).
11. M.M.N. Clyne and J.A. Coxon, Proc. Roy. Soc. (London.) Ser. A 293, 424 (1967).
12. T.Y. Chang, Mol. Phys. 12, 487 (1967).
13. Y.P. Varshini, Rev. Mod. Phys. 29, 664 (1957).
14. R. Rydberg, Z. Physik, 73, 376 (1931).
15. U. Klein, Z. Physik 76, 221 (1932).
16. A.L.G. Rees, Proc. Phys. Soc. (London.) 59, 998 (1947).
17. J.T. Vanderslice, E.A. Mason, W.G. Maisch and E.R. Lippincot, J. Mol. Spectr. 2, 17 (1959), 5, 83 (1960).

18. R.H. Davis and J.T. Vanderslice, *J. Chem. Phys.* 45, 95 (1966).
19. R.H. Davis and J.T. Vanderslice, *Can. J. Phys.* 44, 219 (1966).
20. J. Herzberg, 'Molecular Spectra and Molecular Structure', Vol. I, Spectra of Diatomic Molecules, 2nd Ed. (Van Nostrand, Princeton, 1950).
21. A. Ralston 'A First Course in Numerical Analysis' (McGraw Hill, Kogakusha, Tokyo, 1965).
22. U. Goscinski, *Mol. Phys.* 24, 655 (1972).
23. D. Steele, L.M. Lippincot and J.T. Vanderslice, *Rev. Mod. Phys.* 34, 239 (1962).
24. W.J. Brown, *Phys. Rev.* 33, 1179 (1931), 32, 777 (1932).
25. Y.V. Rao and P. Venkateswarlu, *J. Mol. Spect.* 13, 283 (1964).
26. J.A. Horsley and R.F. Barrow, *Trans. Faraday Soc.* 63, 32 (1967).
27. J.A. Coxon, *J. Mol. Spect.* 37, 55 (1971).
28. R.J. New and G. Burns, *J. Mol. Spect.* 25, 77 (1963).
29. R.F. Barrow, T.J. Clark, J.A. Coxon, and K.K. Yee, *J. Mol. Spect.* 51, 423 (1974).
30. L.L. Albritton, W.J. Marrop, A.L. Schmeltekopf and R.N. Zare, *J. Mol. Spect.* 46, 25 (1973).
31. R.D. Verma, *J. Chem. Phys.* 32, 738 (1960).
32. Y.V. Rao and P. Venkateswarlu, *J. Mol. Spect.* 9, 173 (1962).
33. M.A.A. Clyne and J.A. Coxon, *J. Mol. Spect.* 52, 381 (1976).
34. A.B. Douglas, Chr. An. Möller and S.P. Stoicneff, *Can. J. Phys.* 41, 1174 (1963).

35. A.E. Douglas and A.R. Hoy, Can. J.Phys. 53, 1965 (1975).
36. J.A. Coxon and R. Shankar, J. Mol. Spect. 69, 109 (1978).
37. W.G. Richards and R.F. Barrow, Proc. Chem. Soc. (1962) 297.
38. M.D. Danyluk and G.W. King, Chem. Phys. 25, 343 (1977).
39. R.F. Barrow and A.K. Yee, J. Chem. S. Faraday Trans. II, 69, 684 (1973).
40. J. Tellinghuisen, J & SRT, 19, 149 (1978).
41. J.B. Koffend, R. Bacis and R.W. Field, J. Mol. Spect. 77, 202 (1979).
42. J. Tellinghuisen, M.R. McKeever and A. Sur, J. Mol. Spect. (preprint).
43. A.M. Yee and T.J. Stone, Mol. Phys. 26, 1169 (1973).
44. R. Bacis, S. Chirassw, R.W. Field, J.B. Koffend and J. Verger, J. Chem. Phys. 72, 34 (1980).
45. P. Venkateswarlu, Can. J. Phys. 47, 2525 (1969).
46. V.H. Dibeler, J.A. Walker and A.E. McCulloh, J. Chem. Phys. 53, 4715 (1970).
47. V.H. Dibeler, J.A. Walker, A.E. McCulloh and L.M. Rosenstock, Int. J. Mass. Spectrom. Ion Phys. 7, 209 (1971).
48. A.B. Cornford, D.C. Frost, C.A. McDowell, J.R. Ragle and I.A. Stedhouse, J. Chem. Phys. 54, 2651 (1971).
49. D.C. Frost, C.A. McDowell and D.A. Vroom, J. Chem. Phys. 46, 4255 (1967).
50. C.C. Lu, F.A. Carlson, I.B. Malik, T.C. Jucker and C.V. Westov, Jr., A. Data 3, 1 (1971).